C. R. Physique 20 (2019) 770–802

Contents lists available at ScienceDirect

Comptes Rendus Physique

www.sciencedirect.com

Science in the making 2: From 1940 to the early 1980s / *La science en mouvement 2 : de 1940 aux premières années 1980*

Magnetic structures

Structures magnétiques

Juan Rodríguez-Carvajal [a,*], Jacques Villain [b]

[a] *Diffraction Group, Institut Laue-Langevin, 38054 Grenoble cedex 9, France*
[b] *Theory Group, Institut Laue-Langevin, 38054 Grenoble cedex 9, France*

ARTICLE INFO

Article history:
Available online 26 July 2019

Keywords:
Magnetism
Neutron diffraction
Crystallography
Superspace
Incommensurable structures

Mots-clés :
Magnétisme
Diffraction des neutrons
Cristallographie
Superespace
Structures incommensurables

ABSTRACT

While ferromagnetism has been known since many centuries, more complex magnetic structures have only been identified in the twentieth century: ferrimagnetism, antiferromagnetism, helimagnetism, modulated structures… Incommensurable or long-period structures have first been deduced as consequences of phenomenological models, e.g., the Heisenberg Hamiltonian. The more fundamental explanation of Rudermann, Kittel, Kasuya, and Yoshida relies on the general phenomenon of Friedel oscillations. The coexistence of crystallographic order and magnetic order is sometimes antagonistic and results in sequences of transitions that may be continuous or not. The most effective experimental technique to observe magnetic order is neutron diffraction, but the analysis is sometimes very complicated and requires sophisticated numerical methods involving group theory. In the case of incommensurable structures, it may be useful to consider the three-dimensional system as the section of a higher-dimensional crystal. The determination of magnetic structures from neutron scattering data is facilitated by computers and adequate programs.

RÉSUMÉ

Alors que le ferromagnétisme est connu depuis des siècles, ce n'est qu'au vingtième siècle qu'on identifia des structures magnétiques plus complexes, comme le ferrimagnétisme, l'antiferromagnétisme, l'hélimagnétisme ou les structures magnétiques modulées. La possibilité de structures incommensurables ou à longue période fut d'abord déduite de modèles phénoménologiques tels que le modèle de Heisenberg. L'explication, plus fondamentale, de Rudermann, Kittel, Kasuya et Yoshida repose sur le phénomène général que sont les oscillations de Friedel. L'ordre cristallographique et l'ordre magnétique sont souvent antagonistes, et de leur coexistence résulte souvent une suite de transitions qui peuvent être continues ou non. La technique expérimentale la plus efficace pour l'étude de l'ordre magnétique est la diffraction de neutrons, mais l'analyse est souvent très compliquée et requiert des méthodes numériques élaborées impliquant la théorie des groupes. Dans le cas des structures incommensurables, il peut être intéressant de considérer le système physique tridimensionnel comme la section d'un cristal de

* Corresponding author.
E-mail addresses: jrc@ill.eu (J. Rodríguez-Carvajal), villain@ill.fr (J. Villain).

https://doi.org/10.1016/j.crhy.2019.07.004
1631-0705/

dimension plus élevée. La détermination des structures magnétiques à partir des spectres neutroniques est facilitée par des programmes informatiques appropriés.

1. Introduction: Short history of magnetism

Magnetism has been known since at least 20 centuries, and its application, the compass, has played a major role in the exploration of the Earth since the 16th century. But the only known magnetic phenomenon until the 19th century was ferromagnetism.

In the 19th century, Ampère was able to produce magnetic effects by using electricity. This discovery gave rise to wonderful developments due to Faraday and Maxwell. At the end of the century, Pierre Curie studied paramagnetism and demonstrated that the magnetic susceptibility of paramagnetic salts is proportional to the reciprocal temperature $1/T$ [1]. This experimental Curie law was later derived from statistical mechanics by Paul Langevin [2], whose theory was transcribed in quantum mechanics by Léon Brillouin [3]. The paramagnetism of ferromagnetic materials above the Curie temperature T_C was studied by Pierre Weiss, who proposed a modified Curie law for the susceptibility χ, namely $\chi = C/(T - T_C)$. In 1944, however, Lars Onsager [4] gave an exact treatment of a theoretical model, the two-dimensional Ising model, from which one can deduce, for T close to T_C, the formula $\chi = C/(T - T_C)^\gamma$, where γ is not equal to 1, in contrast with the Curie law. This result was later recognised as general. The exponent γ depends on the dimension of the space and the anisotropy.

In the first half of the twentieth century, it was recognised that certain paramagnetic materials have a magnetic susceptibility that remains finite at all temperatures and has a maximum at a certain temperature, where $\mathrm{d}\chi/\mathrm{d}T$ is discontinuous. The explanation was found by Néel [5]. Néel suggested that the crystal lattice has to be divided into two sublattices, both of which are magnetised, but with two opposite magnetisations. This is *antiferromagnetism*. An example of antiferromagnet is MnO (Fig. 1). Some time later, the possibility of antiferromagnetism was rediscovered by Landau [6], who clarified the concept. At that time, there was no way to check this hypothesis. What was lacking was a diffraction technique able to detect variations of the magnetisation at a scale of the order of a fraction of nanometre. Ten years later, such a technique was available, namely neutron diffraction, and Néel's hypothesis was confirmed by Shull and his coworkers [7,8] in MnO. A long time later, X ray diffraction could also be used [9,10]. X rays, of course, are an electro*magnetic* radiation, but their magnetic scattering turns out to be much weaker than the electric scattering.

More complex magnetic structures may appear in more complex materials. In *ferrimagnetism*, some magnetic moments point in some direction, other moments in the opposite direction, but there is a net magnetic moment. It also happens that the various moments in the unit cell take various directions, not parallel or antiparallel to a particular one [11].

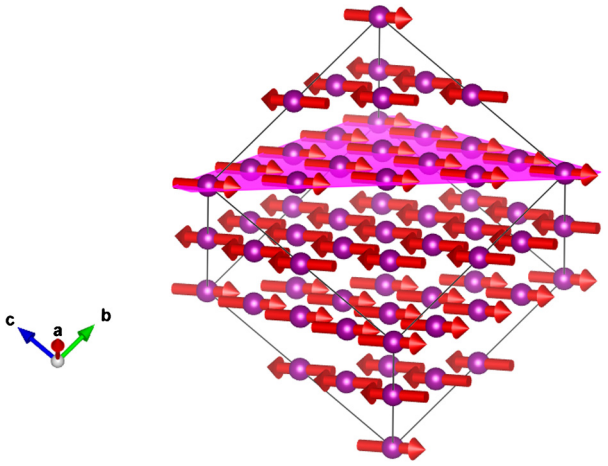

Fig. 1. Magnetic structure of MnO. The circles represent magnetic Mn atoms and the arrows are the corresponding magnetic moments. The middle of the arrows are at the centres of the circles. The structure consists of ferromagnetic layers perpendicular to the [111]-direction of the face-centred cubic unit cell. The represented magnetic unit cell is doubled along the three directions a, b, c with respect to the face-centred cubic unit cell of the paramagnetic, high-temperature phase. Since that cell contains 4 Mn atoms, the magnetic cell represented here contains $4 = 32$ atoms (actually 63 atoms appear on the figure because some of them are on faces, edges, or corners). Actually, the smallest possible unit cell contains 2 atoms and the symmetry is hexagonal. The structure corresponds to formula (7) with $\mathbf{k} = (1/2, 1/2, 1/2)$.

Magnetic materials with a net spontaneous magnetisation, i.e. ferromagnets and ferrimagnets, have important technological applications. Antiferromagnets and more complex structures without net magnetisation have rather few applications.[1] However, physicists want to know and understand all natural phenomena, all properties of matter, and magnetic structures are part of this knowledge. It turns out that their investigation has become a very active branch of solid-state research. Magnetic structures can be very complicated, and the interpretation of experimental data (essentially from neutron scattering) is often a difficult problem.

The next section is devoted to magnetic structures whose period is incommensurable with the crystal lattice (and will be called *incommensurable* without further precision, for brevity). They will be investigated in the framework of the Heisenberg model, which neglects the interaction between magnetism and the lattice. When this interaction is taken into account, serious complications arise, including changes of the period, which will be discussed in section 3. In section 4, a classification of the magnetic structures in terms of the Fourier components of the magnetisation is outlined. The main experimental technique for the study of magnetic structures, namely neutron diffraction, is described in section 5. Section 6 gives examples of complicated magnetic structures with several Fourier components that are not the harmonics of a particular one. Section 7 is devoted to the extension of traditional crystallography and group theory to magnetic materials. This is only possible for commensurable structures, except if the physical, three-dimensional space is viewed as the projection of a space with 4, 5, 6 dimensions or more. This 'superspace' approach is addressed in section 8. The determination of magnetic structures is not always easy, and computers are often useful, as explained in section 9. Technical points are addressed in three appendices.

2. Incommensurable magnetic structures

2.1. Phenomenology

In 1959, one of the authors of the present article (J.V.) was beginning a scientific career at the nuclear research centre of Saclay, one of the few European institutions that had neutrons at their disposal. His advisors were André Herpin, Pierre Mériel, and Pierre-Gilles de Gennes. De Gennes had scientific contacts with a Norwegian physicist, Tormod Riste, and delegated a part of the discussion to his student. Riste was investigating magnetic neutron scattering of a rather complicated magnetic crystal near the transition temperature. De Gennes and his student were supposed to interpret the data, assuming magnetic moments (or spins $\mathbf{S}_l$) localised at the sites l of a lattice and interacting through the so-called Heisenberg Hamiltonian:

$$\mathcal{H} = -(1/2)\sum_{lp} J_{lp}\mathbf{S}_l\cdot\mathbf{S}_p \tag{1}$$

This Hamiltonian had already been used to explain ferromagnetism and antiferromagnetism. It was generally assumed that the coupling constant J_{lp} has a certain value J if l and p are neighbours, otherwise $J_{lp} = 0$. Ferromagnetism is obtained if $J > 0$ and antiferromagnetism if $J < 0$.

The Heisenberg Hamiltonian (1) has the astonishing property to be invariant by any rotation of the whole set of magnetic moments. It is therefore isotropic in the spin space. This is an acceptable approximation in many cases when the magnetism is due to electronic spins while orbital moments are 'quenched' by the crystal field. This is because exchange interactions J_{lp} are a result of the Coulomb interaction (which does not depend on the spin) combined with the Pauli principle (which does not imply any precise spin direction).

However, this isotropy is just an approximation. Generally the main cause of anisotropy is the orbital moment, coupled with the spin according to the Dirac equation. For instance, in Fe, the anisotropy favours magnetisation parallel to a 4-fold axis.

Since Riste's material (magnetite, Fe_3O_4 [13]) was a little complicated, with several magnetic atoms per unit cell, de Gennes' student made more general assumptions and observed that the resulting structure could in certain cases be neither ferromagnetic nor antiferromagnetic, but something else. For instance, if the magnetic atoms form a linear chain, and if the non-vanishing interaction is $J_{lp} = J$ for the nearest neighbours and $J_{lp} = J'$ for the next nearest neighbours, one can consider a helical structure, in which two successive spins make an angle φ. Then the energy is, for N atoms is:

$$W = -N(J\cos\varphi + J'\cos 2\varphi) \tag{2}$$

In the actual structure, the angle φ should minimise this energy. It is straightforward to see that if $J' < 0$ and $|J| < -4J'$, the minimum energy corresponds to a value of φ which is neither 0 (as in ferromagnetism) nor π (as in antiferromagnetism). The magnetic period may be incommensurable with the crystallographic period.

The student went to his master and reported his observation. De Gennes reflected a few seconds before he encouraged his student to develop his idea. Actually, de Gennes had an additional information. Indeed, although he was a theoretician, he knew that, in the same group, Pierre Mériel had obtained the neutron diffraction spectrum of an alloy (the formula of

[1] Recently, antiferromagnets, in form of thin films, have found some applications in *Spintronics* (see for instance [12]).

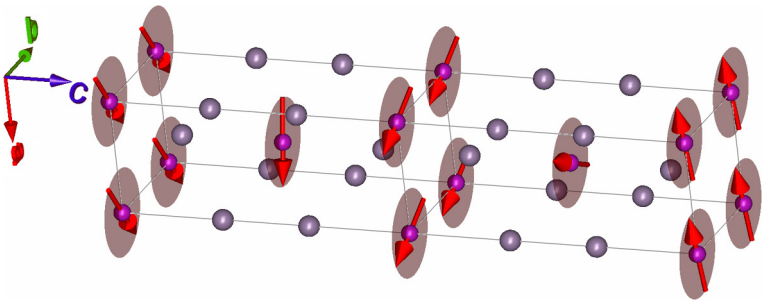

Fig. 2. Magnetic structure of $MnAu_2$ [15]. The pattern is repeated in the two directions perpendicular to the four-fold axis c.

which turned out to be $MnAu_2$) and had found diffraction peaks at completely unexpected positions. This could be due to a magnetic period incommensurable with the crystallographic period. A rather simple calculation confirmed this idea: $MnAu_2$ is a helimagnet, a magnet with a helical magnetic structure.

As the French scientists learned a few months later (from Louis Néel, who was better informed of the current bibliography), they were not the first to remark that the minimisation of the energy (1) could lead to an incommensurable structure. The same observation had already been made by the Japanese Akio Yoshimori [14], a scientist who later made a nice contribution to the understanding of the Kondo effect.

Yoshimori looked for the minimum of the Heisenberg Hamiltonian (1), where the spins $\mathbf{S}_i$ are localised at the sites $\mathbf{R}_i$ of a Bravais lattice. He treated the spins $\mathbf{S}_i$ as classical vectors that all have the same modulus s:

$$|\mathbf{S}_l|^2 = s^2 \tag{3}$$

Instead of imposing this condition, Yoshimori imposed the weaker condition

$$\sum_l |\mathbf{S}_l|^2 = Ns^2 \tag{4}$$

where N is the number of magnetic sites. If we are lucky, the minimum of (1) with condition (4) will satisfy (3) and thus will solve the problem. As will be seen, Yoshimori was lucky.

The minimum of the energy (1) with condition (4) is obtained by introducing a Lagrange multiplier λ, minimising

$$-\sum_{lp} J_{lp}\mathbf{S}_l\cdot\mathbf{S}_p + \lambda\sum_l |\mathbf{S}_l|^2 \tag{5}$$

without any condition, and choosing λ such that (4) is satisfied. The minimum of (5) is given by

$$\sum_p J_{lp}\mathbf{S}_p = \lambda\mathbf{S}_l \tag{6}$$

If the magnetic sites $\mathbf{R}_l$ form a Bravais lattice, it is easily checked that a solution to (6) is[2]

$$\mathbf{S}_l = s\mathbf{u}\cos(2\pi\mathbf{k}\cdot\mathbf{R}_l) + s\mathbf{v}\sin(2\pi\mathbf{k}\cdot\mathbf{R}_l) \tag{7}$$

where $\mathbf{u}$ and $\mathbf{v}$ are two orthogonal unit vectors and $\mathbf{k}$ is a parameter, the so-called *propagation vector*. It turns out that we are lucky, because (7) turns out to satisfy the strong condition (3)! Insertion of (7) into (1) yields the magnetic energy as a function of $\mathbf{k}$ and has to be minimised with respect to $\mathbf{k}$. This minimisation solves the problem. For certain values of the exchange constants J_{lp}, the obtained ground state is incommensurable. This calculation is just a generalisation of the above argument for a linear chain with interactions between nearest and next-nearest neighbours.

Yoshimori had no neutrons at his disposal, and $MnAu_2$ was, to our knowledge, the first incommensurable magnetic structure to be discovered [16]. This discovery was the result of a perfect collaboration between theorists and experimentalists.

A number of other incommensurable magnetic structures were discovered in the following years. Certain elements have such structures: a transition metal, chromium, and many rare earths.

To derive formula (7), the magnetic atoms have been assumed to form a Bravais lattice. How can the theory easily be extended to materials in which there are several magnetic ions per unit cell? Bertaut [17] could derive a very simple equation from the Heisenberg Hamiltonian (1). The equation of motion is

[2] We will normally use the crystallographic convention in which the $\mathbf{k}$-vectors are referred to the reciprocal space in which the coordinates are referred to the reciprocal basis $\mathbf{a}_j^*$ $(j = 1, 2, 3)$ satisfying the relations: $\mathbf{a}_i\mathbf{a}_j^* = \delta_{ij}$. If the $\mathbf{a}_i$ vectors describe a primitive basis, the reciprocal lattice, generated by integer linear combinations of $\mathbf{a}_j^*$, is denoted by L^*. In solid-state physics, the reciprocal lattice is defined as $\mathbf{a}_i\mathbf{b}_j = 2\pi\delta_{ij}$, so that $\mathbf{b}_j = 2\pi\mathbf{a}_j^*$. If the factor 2π does not appear in the exponentials in some parts of this work, it is understood that we are using the solid-state physics convention.

$$\hbar\, \mathrm{d}\mathbf{S}_l/\mathrm{d}t = \sum_p J_{lp}\mathbf{S}_p \times \mathbf{S}_l$$

At equilibrium, there is no motion, $\mathrm{d}\mathbf{S}_i/\mathrm{d}t = 0$ and therefore

$$\sum_p J_{lp}\mathbf{S}_p = \lambda_l \mathbf{S}_l \tag{8}$$

With a single magnetic ion per unit cell, λ_l is independent of l as proved above at zero temperature. In more complex cases the solution to Bertaut's equation (8) is not so easy. The symmetry of the coefficient λ_l has been discussed by Bertaut [18].

2.2. Microscopic theory of incommensurable magnetism

The theory we developed in Saclay [19] was based on formula (1), which was purely phenomenological. Why should the interaction J' between next-nearest neighbours be particularly large?

The Saclay group had done a rather good job, except for a tremendous ignorance of recent progress in theoretical physics. In 1954, Rudermann and Kittel had given a theory of exchange between localised spins in metals, which provided a long-range interaction with an oscillating behaviour as a function of distance. Their theory is summarised in this section and details are given in Appendix A. In the theory, there are conduction electrons with spin $\sigma = 1/2$ or $-1/2$, associated with creation and destruction operators $c^+_{k\sigma}$ and $c_{k\sigma}$ in the reciprocal space, $c^+_{l\sigma}$ and $c_{l\sigma}$ in the direct space. And there are N localised spins $\mathbf{S}_i$. We assume that there is one spin per unit cell.

The Hamiltonian contains two parts: i) the kinetic energy of the free electrons, and ii) a local, magnetic interaction between any localised spin and the conduction electron(s), which turn out to be present on the same atom as the localised spin. This interaction arises from the Pauli principle combined with the electrostatic repulsion between electrons, as originally realised by Heisenberg [20]. The same interaction is responsible for Hund's rule in atoms.

When conduction electrons are treated in second-order perturbation theory, Rudermann and Kittel [21] obtained an interaction between localised spins that has the form of a Heisenberg Hamiltonian (1) with an interaction J_{ij} which is a long-ranged, oscillating function $J(R_{ij})$ of the distance R_{ij}:

$$J(\mathbf{R}) = J(R) = \frac{A}{R^3}\cos(2k_\mathrm{F}R) \tag{9}$$

The reason for the oscillations is the same as that for Friedel oscillations in the charge density around an impurity in a metal: both phenomena are the result of the sharp discontinuity (at temperature $T = 0$) of the occupation of electronic states at the Fermi level.

To obtain formula (9), a spherical Fermi surface should be assumed. In the realistic case of a non-spherical Fermi surface, the calculation is more complicated, but Friedel oscillations are still there. The relevant bibliography will be found in the reviews published in 2016 as a tribute to Jacques Friedel [22–25].

At nonvanishing temperature, the oscillations are damped at very long distance, but the oscillating character at moderate distances explains the helical structures observed especially in rare earths [26].

3. Magnetic interactions

3.1. General features

As stated above, the isotropic Hamiltonian (1) is an acceptable approximation in many cases when the magnetism is due to electronic spins while orbital moments are 'quenched' by the crystal field.

However, this isotropy is just an approximation. Magnetic dipole interactions are perhaps the most obvious anisotropy, but generally the main cause of anisotropy is the orbital moment, coupled with the spin according to the Dirac equation. For instance, in Fe, the anisotropy favours magnetisation parallel to a 4-fold axis. The strength of the anisotropy in a cubic crystal depends on temperature and vanishes at the Curie point.

If the anisotropy is very strong, and favours a particular crystallographic axis, all moments should be parallel to this axis, and this favours ferro-, ferri-, or antiferromagnetism, especially at low temperature. At non-vanishing temperature, the anisotropy turns out to be less effective and incommensurable, or long-period 'modulated' structures are possible. A remarkable case is that of the alloy CeSb, which has a sequence of phase transitions (Fig. 3) with various periods when the temperature changes [27]. Seven different phases have been observed at different magnetic fields and temperatures, in addition to the paramagnetic phase and the ferromagnetically ordered phase in very strong field. The transitions are discontinuous, or 'first order' in the language of physicists.

Are they always discontinuous? No! In certain cases, the (theoretical) phase diagram has very strange mathematical features, as will now be seen.

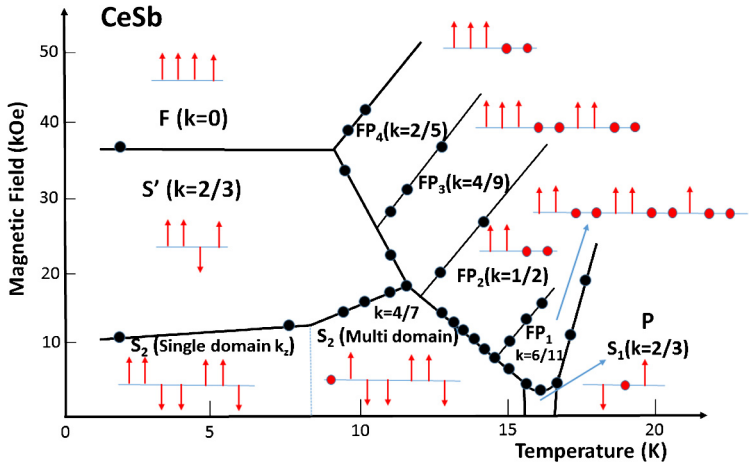

Fig. 3. Magnetic phase diagram of CeSb under an applied magnetic field. The picture has been prepared after Rossat-Mignod et al. [28]. The structure is a stacking of planes with positive magnetisation, negative magnetisation, and almost vanishing magnetisation, represented respectively by up arrows, down arrows, and dots.

3.2. The Devil's staircase

Instead of treating the Hamiltonian (1) we consider here a model which also gives rise to incommensurable and long period structures.

We start with a one-dimensional chain of magnetic moments $\mathbf{S}_n$ with an easy magnetisation plane. The index n takes the values $n = 1, 2, 3, \ldots, N$ and the case of interest is the limit $N \to \infty$. In practice, the moments $\mathbf{S}_n$ can be the magnetisations of the successive layers of a three-dimensional material, as the alloy $MnAu_2$ studied in section 2. The n-th moment has two components, which may be called $s\cos\varphi_n$ and $s\sin\varphi_n$. The energy is assumed to have the form

$$\mathcal{H} = -D\sum_n \cos(\varphi_{n+1} - \varphi_n - \mu) - \lambda\sum_n \cos\varphi_n \tag{10}$$

where D, λ, and μ are positive constants. The first term is an exchange interaction that does exist in certain materials [29, 30]. The second term appears if an external magnetic field is applied. A similar term with $\sum\cos 2\varphi_n$ or $\sum\cos 4\varphi_n$ instead of $\sum\cos\varphi_n$ might result from an in-plane anisotropy. If μ and λ are not too large, the first cosine can be approximately replaced by its Taylor expansion limited to the quadratic term. One now obtains the so-called discrete Frenkel–Kontorova model [31]

$$\mathcal{H} = \sum_n \left[\frac{1}{2}(\varphi_{n+1} - \varphi_n)^2 - \mu(\varphi_{n+1} - \varphi_n)\right] - \lambda\cos\varphi_n \tag{11}$$

where D has been set equal to $1/2$, as is allowed by a suitable choice of the units. This model has been investigated in detail by several authors, and particularly by Serge Aubry [32]. Although it does not seem to be appropriate for magnetism, its qualitative properties are presumably analogous to those of the magnetic model (10).

The problem is to find the minimum of (11).

Expressions (10) and (11) can represent the free energy of a three-dimensional system as a function of the magnetisations of the successive layers. The minimisation of these expressions will then provide the equilibrium magnetic structure as a function of temperature, if the temperature dependence of D, λ, and α is known. However, the temperature is generally not considered in the theoretical treatment [32]. Theorists prefer to study the evolution of the average angle $\Delta = (\varphi_N - \varphi_1)/(N-1)$ when μ varies. The physical cause of this variation (temperature, pressure…) will not be addressed here.

When $\lambda = 0$, the minimum of (11) obviously corresponds to $\varphi_{n+1} - \varphi_n = \mu$ for all values of n, and therefore $\Delta = \mu$. When λ is not 0, the evolution is much more complicated [32]. It turns out that all rational values p/q of Δ/π minimise (11) in a non-vanishing interval $[\mu_{pq}^-, \mu_{pq}^+]$. A justification of this statement is given in Appendix B. The resulting structure is periodic: $\varphi_{n+2q} = \varphi_n + 2p\pi$.

Thus the curve $\Delta(\mu)$ contains a sequence of horizontal parts, where $\mathrm{d}\Delta/\mathrm{d}\mu = 0$. It looks like a staircase. But, unlike usual staircases, it is continuous! Indeed, given any rational number, it is always possible to find another rational number closer to it than any arbitrarily small positive number. Such a strange curve has been called *Devil's staircase* by Benoît Mandelbrot.

A particularly strange property of certain Devil's staircases is that they can be *complete*, i.e. horizontal almost everywhere, so that $\mathrm{d}\Delta/\mathrm{d}\mu = 0$ almost everywhere.

In Appendix B, certain of the above-described properties are justified. The infinite sequence of continuous transitions, called Devil's staircase, is by no means a general property of incommensurable magnetism. Staircases of first-order transition also exist in magnetism [33]. An example is given by the above-mentioned material CeSb.

The Devil's staircase seems to be essentially a theoretical concept, whose experimental observation would be very difficult. If one wishes to observe a structure of very long period, this involves a reorganisation of the crystal on a very long scale and this requires a very long time, since discommensurations have to jump over potential barriers. Moreover, the Devil's staircase is a property of pure crystals, and it is not clear whether it survives in the presence of impurities. Nevertheless, it is important to know the theoretical ground state of a pure crystal, or its theoretical equilibrium state at non-vanishing temperature.

3.3. Coexistence of magnetic and crystallographic order: the general case

In the preceding subsection, the crystallographic order which has been taken into account was particularly simple: a succession of identical planes. We now wish to understand how magnetism can match any crystallographic structure. Then each atom is characterised by its unit cell and by its position in this unit cell. Unit cells will be labelled by the indices $l, m, n, l', m' \ldots$, which can take an arbitrarily large number N of values. The position in the unit cell will be labelled by the indices $i, j, i', j' \ldots$, which can take a finite number of values, which depends on the material of interest. With these notations, the vector position of the atom i in the unit cell l is $\mathbf{R}_{il} = \mathbf{R}_l + \mathbf{r}_i$. Since each magnetic moment or 'spin' has three components x, y, z, denoted by indices like α, β, α', β', their components $S_{il\alpha}$ are labelled by three indices. The most general Hamiltonian in the absence of external magnetic field will be assumed to have the following form:

$$H = -\sum_{il\alpha,\, jm\beta} J^{\alpha\beta}_{il,\,jm} S_{il\alpha} S_{jm\beta} + \sum_{il\alpha,\, jm\beta,\, i'l'\alpha',\, j'm'\beta'} J^{\alpha\beta\alpha'\beta'}_{il,\,jm,\,i'l',\,j'm'} S_{il\alpha} S_{jm\beta} S_{i'l'\alpha'} S_{j'm'\beta'} + \ldots\ O(S^{2n}) \tag{12}$$

In the presence of a magnetic field, odd terms should be added.

As in the previous sections, the spins are assumed to be classical vectors.[3] If we consider that the magnetic atoms at positions $\mathbf{R}_{il}$ have intrinsic magnetic moments of modulus m_i ($\mathbf{S}_{il} = m_i \mathbf{n}_{il}$), for a given set of exchange parameters $J^{\alpha\beta}_{il,\,jm}, J^{\alpha\beta\alpha'\beta'}_{il,\,jm,\,i'l',\,j'm'}, \ldots$, the magnetic structure at $T = 0$ K corresponds to the minimum of H with respect to the orientations of the unit vectors $\mathbf{n}_{il}$. In general, the terms of order greater than 2 in the spins are much weaker than those of second order. Moreover, the isotropic part of the tensors $J^{\alpha\beta}_{il,\,jm}$ is strongly dominant in many cases; the energy can be simplified to obtain the so-called Heisenberg Hamiltonian (1). Taking into account explicitly the two kinds of indices $i, j, i', j' \ldots$ and $l, m, l', m' \ldots$, formula (1) reads

$$\begin{aligned} H_{iso} &= -\sum_{il,\,jm} J_{il,\,jm} \mathbf{S}_{il} \cdot \mathbf{S}_{jm} = -\sum_{il,\,jm} J_{ij}(\mathbf{R}_m - \mathbf{R}_l) \mathbf{S}_{il} \cdot \mathbf{S}_{jm} \\ H_{iso} &= -\sum_{il,\,jm} J_{ij}(\mathbf{R}_m - \mathbf{R}_l) m_i m_j \mathbf{n}_{il} \cdot \mathbf{n}_{jm} = -\sum_{il,\,jm} J_{ij}(\mathbf{R}_m - \mathbf{R}_l) m_i m_j \cos\theta_{il,\,jm} \end{aligned} \tag{13}$$

As stressed in section 2, the magnetic energy in such a case does not depend on the absolute orientation of the spins. It depends only on the relative orientation of the spins (scalar product). This means that, for a given configuration, any global rotation acting on the spins does not change the energy, so the Hamiltonian has more symmetry elements than the space group underlying the crystal structure if the interaction between magnetic moments is strictly isotropic.

Even restricting to the quadratic terms of (12), the determination of the classical ground state of a system in which we know the exchange interaction parameters is a task that cannot be solved analytically, except for very simple cases (Bravais lattices [14,22], linear chain [34]). In general, numerical Monte Carlo simulations are needed for determining the ground state or a configuration very close to it. A simpler case is the determination of the so-called *first ordered state*, which is the spin configuration appearing just below the order temperature. The study of the resolution of these two problems started at the middle of the fifties in the last century by several authors [34–37]. In Appendix C, we present the mean-field approximation for classical spins to determine the first ordered state in a way similar to that of Freiser [34], resulting in equations formally equivalent to (8).

We see here that the relevant symmetry to be considered for studying the magnetic ordering is that of the system Hamiltonian. However, the Hamiltonian of a system is generally unknown, so we do not know what is the relevant symmetry to begin with. In the absence of this information, we have at our hands the possibility to know the crystal structure symmetry of the compound under study. The space group of the crystal summarises in some way the result of different interactions

[3] A quantum description generally does not modify the qualitative features of the magnetic structure. However, the mean spin value at zero temperature is reduced in antiferromagnets by quantum fluctuations [38,39]. Also, one can go beyond the mean field approximation, using for instance the Renormalisation Group technique. This modifies the temperature dependence of the physical quantities such as susceptibility or magnetisation, but this does not essentially modify the magnetic structures.

between electrons and nuclei in the solid. We expect that the magnetic ordering conserves some of the symmetry properties of the crystallographic structure, even in the case of a structural transition accompanying the magnetic ordering. This is the reason why we use the crystal structure symmetry as a starting point for our analysis and the basis for applying the representation method introduced by Bertaut [40]. In the course of experimental data analysis for determining a magnetic structure, we may arrive to the conclusion that we have to modify our previous assumptions on the starting symmetry, or even to suppose that we have additional symmetry elements in the magnetic Hamiltonian than in the crystallographic space group.

4. Description of magnetic structures using the concept of propagation vector. General types of magnetic structure

A magnetic structure is defined by the average magnetisation (in units of Bohr magnetons: μ_B) $\mathbf{m}_{jl}$ of the magnetic ion j of the l-th unit cell. The average is over thermal and quantum fluctuations.

When there is a single magnetic atom per unit cell, the ground state of (1) is given by (7) for classical spins. At finite temperature and when quantum corrections are taken into account, the magnetic structure is still given by a formula analogous to (7), where the spin modulus s is just replaced by a function of temperature and s. When there are several magnetic atoms per unit cell and when anisotropy is taken into account, the magnetic structure of any crystal is given by the following generalisation of (7) [41]:

$$\mathbf{m}_{jl} = \sum_{\mathbf{k}} \mathbf{S}_{\mathbf{k}j} \exp(-2\pi i \mathbf{k}\cdot\mathbf{R}_l) \tag{14}$$

The main change with respect to (7) is that there is a summation on the 'propagation vectors' $\mathbf{k}$. When there are several propagation vectors, they are frequently members of the same *star*, i.e. of the set of $\mathbf{k}$-vectors deduced from one of them by the symmetry operations of the underlying point group (see section on representation analysis 7.1, point 2). However, this summation is often limited to a single term corresponding to a single propagation vector, which may be 0 (case a discussed below) or half a reciprocal lattice vectors (case b below). In other cases (case c), the anisotropy generally introduces harmonics, e.g., multiples $2\mathbf{k}$, $3\mathbf{k}$, etc. of a 'primary' propagation vector $\mathbf{k}$. Very often, there is a single primary propagation vector, but there may be two or three primary propagation vectors.

In (14), any vector $\mathbf{k}$ may be replaced by $\mathbf{k}+\mathbf{H}$, where $\mathbf{H}$ is any reciprocal lattice vector. Since $\mathbf{H}$ can be chosen such that $\mathbf{k}+\mathbf{H}$ is in the first Brillouin zone, all vectors $\mathbf{k}$ in (14) may be assumed to be in the first Brillouin zone. So $\mathbf{k}$-vectors are at the interior (*IBZ*) or in the surface of the Brillouin zone.

The Fourier coefficients $\mathbf{S}_{\mathbf{k}j}$ are, in general, complex vectors and must verify the equality $\mathbf{S}_{-\mathbf{k}j} = \mathbf{S}^*_{\mathbf{k}j}$ because the vectors $\mathbf{m}_{jl}$ are real.

Let us describe general types of magnetic structures of increasing degree of complexity using formula (14).

a) The simplest types of magnetic structures existing in complex crystals have a single null propagation vector at the centre of the first Brillouin zone: $\mathbf{k} = (0,0,0) = \mathbf{0}$. The Fourier coefficients should be real and can be identified with the magnetic moments directly:

$$\mathbf{m}_{jl} = \mathbf{S}_{\mathbf{0}j} \exp(-2\pi i \mathbf{0}\cdot\mathbf{R}_l) = \mathbf{S}_{\mathbf{0}j} = \mathbf{m}_{\mathbf{0}j} \tag{15}$$

This expression tells us that the orientation and magnitudes of the magnetic moments in whatever cell of the crystal are identical to those of the zero-cell. The translational symmetry of the magnetic structure is identical to that of the crystal structure: the magnetic unit cell is the same as the chemical cell. This class of magnetic structures may be ferromagnetic, ferrimagnetic, or antiferromagnetic, collinear or non-collinear. A vanishing propagation vector does not imply a ferromagnetic structure. This is only true for Bravais lattices (a single magnetic atom per primitive cell). Examples of $\mathbf{k} = \mathbf{0}$ magnetic structures are shown in Fig. 4 (collinear) and in Fig. 5 (non-collinear).

b) The next class of magnetic structures corresponds also to a single propagation vector, in this case of the form: $\mathbf{k} = \mathbf{H}/2$, where $\mathbf{H}$ is a reciprocal lattice vector. There is a single term in (14) because, by definition, $\mathbf{k} \equiv -\mathbf{k}$. The propagation vectors of this kind correspond to high symmetry points of the surface of the BZ. In this case, we have:

$$\mathbf{m}_{lj} = \mathbf{S}_{\mathbf{k}j} \exp(-\pi \mathrm{i} \mathbf{H}\cdot\mathbf{R}_l) = \mathbf{S}_{\mathbf{k}j} (-1)^{\mathbf{H}\cdot\mathbf{R}_l} = \mathbf{m}_{\mathbf{0}j} (-1)^{n_l} \tag{16}$$

This expression tells us that the orientation and magnitudes of the magnetic moments in whatever cell of the crystal are either identical or opposite to those of the zero-cell. The translational symmetry is lower than that of the chemical cell. The magnetic cell can easily be deduced from the particular values of the propagation vector (see [43] for a classification of magnetic lattices in terms of propagation vectors). The magnetic structures of this kind are necessarily antiferromagnetic. An example is the case of MnO (the first determined magnetic structure using neutron diffraction!) represented in Fig. 1.

c) A third class of magnetic structures corresponds the general case, where the $\mathbf{k}$-vector is not a special vector as in the two previous classes. The $\mathbf{k}$-vectors are then at the interior of the first Brillouin zone in a general position (non-rational components of $\mathbf{k}$). The general expression of the Fourier coefficient for the atom j is explicitly given by:

$$\mathbf{S}_{\mathbf{k}j} = \frac{1}{2}\{\mathbf{R}_{\mathbf{k}j} + \mathrm{i}\,\mathbf{I}_{\mathbf{k}j}\} \exp(-2\pi \mathrm{i} \phi_{\mathbf{k}j}) \tag{17}$$

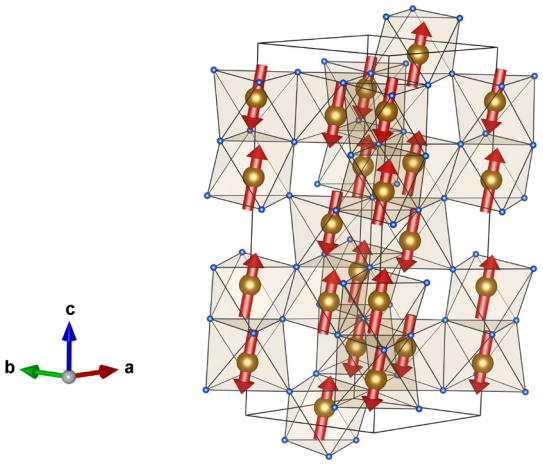

Fig. 4. Antiferromagnetic structure of hematite α-Fe_2O_3 at 10 K. The moments are nearly parallel to the c-axis. An additional weak ferromagnetic component is neglected in this collinear model [42]. Above about 250 K, the moments become parallel to the a-axis (Morin transition).

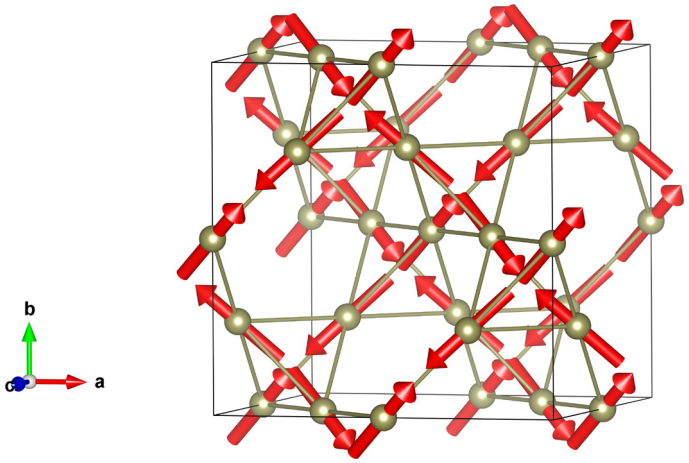

Fig. 5. Magnetic structure of the pyrochlore $Tb_2Sn_2O_7$. For each tetrahedron of Tb atoms, there are two moments pointing towards the centre of the tetrahedron and two moments pointing out of the centre. This is a non-collinear magnetic structure with $\mathbf{k} = (0, 0, 0)$: the crystallographic unit cell is identical to the magnetic unit cell [44].

Only six real parameters define the $\mathbf{S}_{\mathbf{k}j}$ vectors, so the phase factor $\phi_{\mathbf{k}j}$ is not generally needed if the three components of $\mathbf{R}_{\mathbf{k}j}$ and the three components of $\mathbf{I}_{\mathbf{k}j}$ are arbitrary, but it is convenient to use it when particular relations or constraints between real vectors, $\mathbf{R}_{\mathbf{k}j}$ and $\mathbf{I}_{\mathbf{k}j}$, are given (see below). The calculation of the magnetic moment of the atom j in the unit cell of index l, should be performed by using the formula (14) that may be also written in this case as:

$$\mathbf{m}_{jl} = \sum_{\langle \mathbf{k} \rangle} \mathbf{R}_{\mathbf{k}j} \cos 2\pi[\mathbf{k}\mathbf{R}_l + \phi_{\mathbf{k}j}] + \mathbf{I}_{\mathbf{k}j} \sin 2\pi[\mathbf{k}\mathbf{R}_l + \phi_{\mathbf{k}j}] \tag{18}$$

where the sum is now extended to half the number of propagation vectors, i.e. over the total number of pairs $\mathbf{k}$, $-\mathbf{k}$ and their harmonics.

If the magnetic structure represents a helical/spiral order there is only a single pair $\mathbf{k}$, $-\mathbf{k}$ and the Fourier coefficients are of the form:

$$\mathbf{S}_{\mathbf{k}j} = \frac{1}{2}[m_{1j}\mathbf{u}_j + \mathrm{i}m_{2j}\mathbf{v}_j] \exp\{-2\pi \mathrm{i}\phi_{\mathbf{k}j}\} \tag{19}$$

where $\mathbf{u}_j$ and $\mathbf{v}_j$ are orthogonal unit vectors, forming a plane. Notice that these unit vectors together with $\mathbf{w}_j = \mathbf{u}_j \times \mathbf{v}_j$ define an orthogonal reference system with origin at the atom j; its orientation in space is determined by three Euler angles that, together with m_{1j}, m_{2j} and $\phi_{\mathbf{k}j}$, completes the 6 parameters per atom defining the Fourier coefficients $\mathbf{S}_{\mathbf{k}j}$. From Fourier coefficients like in equation (19) and disregarding the harmonics of $\mathbf{k}$, three situations can be considered.

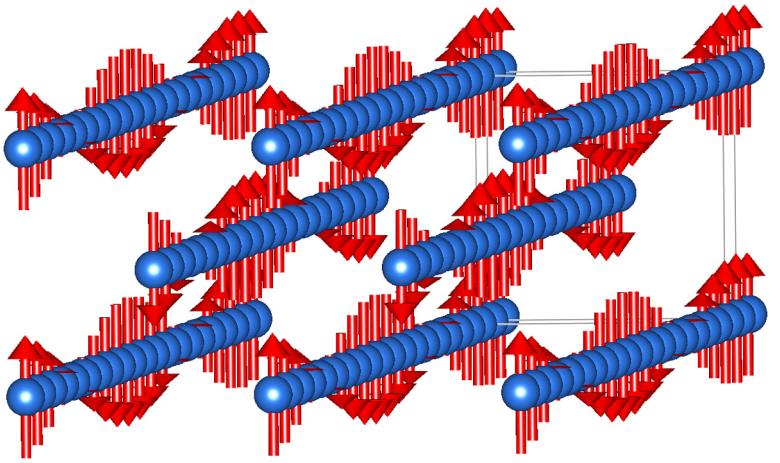

Fig. 6. Magnetic structure of the metallic solid element Cr [45,46]; a perspective view. The blue circles are Cr atoms and the red arrows represent the magnetic moments. The length of each arrow is proportional to the corresponding moment.

1. If $m_{2j} = 0$ (or $m_{1j} = 0$), the magnetic structure corresponds to a modulated sinusoid of amplitude m_{1j} (or m_{2j}). An example of sinusoidal structure is that of the spin-density wave observed in metallic Cr [45,46] and represented in Fig. 6.
2. If $m_{1j} = m_{2j} = m_0$ and the propagation vector is perpendicular to the plane ($\mathbf{u}_j$, $\mathbf{v}_j$), the magnetic structure for the sublattice j corresponds to a classical helix (or spiral) with cylindrical envelope. If the propagation vector is within the ($\mathbf{u}_j$, $\mathbf{v}_j$) plane, the structure is called a cycloid. In both cases, all j atoms have a magnetic moment equal to m_0. An example of this kind of structure is that of $MnAu_2$ [16] represented in Fig. 2.
3. If $m_{1j} \neq m_{2j}$, the helix (or cycloid) has an elliptical envelope and the moments have values between $\min(m_{1j}, m_{2j})$ and $\max(m_{1j}, m_{2j})$. A recent example of this kind of magnetic structure (cycloidal structure) is that of $TbMnO_3$ in the temperature range $10\ \text{K} < T < 28\ \text{K}$ [47].

5. Determination of magnetic structures using neutron diffraction

The scattering of neutrons by matter results from two interactions: i) the strong nuclear interaction with nuclei, ii) the magnetic dipole interaction between the neutron spin and the magnetic moment of unpaired electrons. Such electrons are only present in the outer electronic shell of magnetic ions, such as transition metals, rare earths, or actinides. This electronic moment results from the spin and from the orbital moment. In certain cases, however, there is no orbital moment, for instance in Fe^{3+} and Mn^{2+}, which have 5 electrons on the 3D shell. In other cases, the orbital moment is 'quenched' by the crystal field, and therefore negligible.

The information obtained from neutron scattering is not always sufficient to derive the magnetic structure. The information is more complete if polarised neutrons are used and if the polarisation of scattered neutrons is analysed [48–51].

5.1. Neutron scattering cross sections and magnetic structure factor

In a neutron diffraction experiment, a beam of neutrons with momentum $\hbar\mathbf{k}_I$ is diffracted by a crystal and the number of neutrons with momentum $\hbar\mathbf{k}_F = \hbar(\mathbf{k}_I + \mathbf{Q})$ is measured. The vector $\mathbf{Q}$ is called the scattering vector (crystallographers prefer to use the vector $\mathbf{h} = \mathbf{Q}/2\pi$). The diffracted wave function is the sum of a nuclear part $N_\mathbf{h}$ (resulting from nuclear scattering) and a magnetic part, which is the relevant one to determine the magnetic structure. This magnetic part depends on a vector $\mathbf{M}(\mathbf{h})$ which may be roughly defined as the 3-dimensional Fourier transform of the magnetisation density. In an infinite crystal, the nuclear structure factor $N_\mathbf{h}$ and the magnetic structure factor $\mathbf{M}(\mathbf{h})$ vanish, except for a discrete set of vectors $\mathbf{h}$ (Bragg peaks). In an antiferromagnet, there are pure magnetic reflections with $N_\mathbf{h} = 0$, pure nuclear reflections with $\mathbf{M}(\mathbf{h}) = \mathbf{0}$, and mixed reflections containing both contributions. The intensity of magnetic Bragg peaks due to neutron scattering by magnetically ordered systems can be calculated in a similar way as for X-rays or nuclear neutron scattering. X-ray diffraction measures the modulus of the Fourier transform of the electronic density. Analogously, magnetic neutron scattering is sensitive to the Fourier transform of the magnetisation density, which is related to the density of unpaired electrons in atoms.

Here we follow some sections of the reference [41]. We summarise the most important expressions needed to calculate the intensity of a Bragg reflection; the reader interested in more details about elastic magnetic scattering in relation with magnetic structures can consult [28,52] and the references therein. The interaction of neutrons with the magnetic moments of atoms is of dipolar origin through the magnetic moment of the neutron. The scattering amplitude is then a vector that, for a single atom with atomic moment $\mathbf{m}$, is given by:

$$\mathbf{a}(\mathbf{h}) = pf(h)\mathbf{m}_\perp \tag{20}$$

where $h = |\mathbf{h}|$, $\mathbf{m}_\perp = \mathbf{h} \times (\mathbf{m} \times \mathbf{h})/h^2$ is the perpendicular component of the atomic moment to the scattering vector $\mathbf{h}$ and $p = r_e\gamma/2 = 0.2695 \times 10^{-14}$ m/μ_B, where $r_e = e^2/(4\pi\epsilon_0 mc^2) = 2.8 \times 10^{-15}$ m is the so-called classical radius of the electron and $\gamma = 1.9132\,\mu_N$ (μ_N = nuclear magneton) is the magnetic moment of the neutron. The cross section is then $d\sigma/d\Omega = |\mathbf{a}(\mathbf{h})|^2$. The dimensionless function $f(h)$ is the atomic magnetic form factor (Fourier transform of the unpaired electron density, normalised as $f(0) = 1$, assumed to be spherical hereafter).

In a crystal, there are many atoms with diversely oriented moments $\mathbf{m}_{jl}$. Each of them has a vector scattering length given by (20) and the sum is the total scattering amplitude

The elastic intensity scattered by a crystal, as a function of $\mathbf{h}$, is proportional to the square of the total amplitude (also-called *magnetic interaction vector*):

$$\mathbf{M}_\perp^\tau(\mathbf{h}) = p\sum_{jl} f_j(h)\mathbf{m}_{\perp jl}\exp\{2\pi i\mathbf{h}\cdot\mathbf{R}_{jl}\} = \frac{1}{h^2}\mathbf{h}\times\mathbf{M}^\tau(\mathbf{h})\times\mathbf{h} \tag{21}$$

The total diffraction intensity (cross section) is proportional to the square of this expression. The vector $\mathbf{M}^\tau(\mathbf{h})$ is the magnetic structure factor of the whole crystal. The scattered intensity is calculated as usual by multiplying the above expression by its complex conjugate. Developing the expression of $\mathbf{M}^\tau(\mathbf{h})$ for the case of an ordered magnetic crystal in which the distribution of magnetic moments is given by the equation (14) and separating the sums over the lattice and over the atoms within a unit cell, we obtain:

$$\mathbf{M}^\tau(\mathbf{h}) = p\sum_{jl} f_j(h)\mathbf{m}_{jl}\exp\{2\pi i\mathbf{h}\cdot\mathbf{R}_{jl}\} = p\sum_j f_j(h)\exp\{2\pi i\mathbf{h}\mathbf{r}_j\}\sum_{\mathbf{k}}\mathbf{S}_{\mathbf{k}j}\sum_l \exp\{2\pi i(\mathbf{h}-\mathbf{k})\cdot\mathbf{R}_l\}$$

or

$$\mathbf{M}^\tau(\mathbf{h}) = p\sum_j f_j(h)\exp\{2\pi i\mathbf{h}\mathbf{r}_j\}\sum_{\mathbf{k}}\mathbf{S}_{\mathbf{k}j}\sum_{\mathbf{H}}\delta(\mathbf{h}-\mathbf{k}-\mathbf{H}) \tag{22}$$

This formula indicates that the magnetic intensity is practically zero in the whole reciprocal space, except at positions given by:

$$\mathbf{h} = \mathbf{H} + \mathbf{k} \tag{23}$$

Magnetic diffraction appears like a filter, producing *satellites* around the nuclear reflections characterised by the reciprocal lattice vector $\mathbf{H}$. Each satellite is decoupled from the rest of the satellites, so, if there are different propagation vectors $\mathbf{k}$, there is no interference between them. Notice that the concept of *fundamental* reflections (used in the context of modulated crystal structures) does not apply here because $\mathbf{h} = \mathbf{H}$ corresponds to nuclear reflections. Only when $\mathbf{k} = 0$, there is a magnetic contribution on top of the nuclear reflections. For a particular magnetic reflection indexed as in (23) the magnetic structure factor of the unit cell, having n_c magnetic atoms, is:

$$\mathbf{M}(\mathbf{h} = \mathbf{H}+\mathbf{k}) = \mathbf{M}_\mathbf{h} = p\sum_{j=1}^{n_c} f_j(h)\mathbf{S}_{\mathbf{k}j}\exp\{2\pi i\mathbf{h}\mathbf{r}_j\} = p\sum_{j=1}^{n_c} f_j(h)\mathbf{S}_{\mathbf{k}j}\exp\{2\pi i(\mathbf{H}+\mathbf{k})\mathbf{r}_j\} \tag{24}$$

The intensity of a magnetic Bragg reflection is proportional to the square of the magnetic interaction vector of the unit cell:

$$\mathbf{M}_\perp(\mathbf{h}) = \mathbf{M}_{\perp\mathbf{h}} = \frac{1}{h^2}\mathbf{h}\times\mathbf{M}_\mathbf{h}\times\mathbf{h} = \mathbf{e}\times\mathbf{M}_\mathbf{h}\times\mathbf{e} = \mathbf{M}_\mathbf{h} - (\mathbf{e}\cdot\mathbf{M}_\mathbf{h}) \tag{25}$$

where $\mathbf{e} = \mathbf{h}/|\mathbf{h}|$ is the unit vector along the scattering vector $\mathbf{h}$ given by (23). The intensity of a Bragg reflection for non-polarised neutrons is given by:

$$I_\mathbf{h} = N_\mathbf{h}N_\mathbf{h}^* + \mathbf{M}_{\perp\mathbf{h}}\cdot\mathbf{M}_{\perp\mathbf{h}}^* \tag{26}$$

The problem of determining the magnetic structure of a crystalline solid, for which the crystal structure is known, reduces to the determination of the quantities $\mathbf{k}$ and $\mathbf{S}_{\mathbf{k}j}$ from which we can apply the expression (14) for determining the magnetic moment of whatever atom in the crystal. This result takes into account only the translational symmetry of the crystal. In general, we have enough information from the whole symmetry of the crystal structure to further reduce the number of free independent parameters, and this is the topic of symmetry analysis tackled below. Magnetic neutron diffraction experiments provide as immediate information the position of magnetic reflections in reciprocal space. This allows the determination of the propagation vector(s) characterising the magnetic moment configuration given by the Fourier series (14). The measurement of intensities gives us a list of non-linear equations with the Fourier coefficients $\mathbf{S}_{\mathbf{k}j}$ as unknowns, equations (24) and (26).

In addition to their wave vector $\mathbf{k}_l$, the incident neutrons are characterised by their polarisation $\mathbf{P}$, defined as twice the average value of the spin of the neutrons. For unpolarised neutrons, $\mathbf{P} = 0$. For completely polarised neutrons, $|\mathbf{P}| = 1$. The diffracted intensity when considering polarised incident neutrons and the polarisation of scattered neutrons, $\mathbf{P}_s$, are given by the so-called Blume–Maleyev equations [49,50]:

$$I_{\mathbf{h}} = N_{\mathbf{h}} N^*_{\mathbf{h}} + N_{\mathbf{h}}\{\mathbf{P}\cdot\mathbf{M}^*_{\perp\mathbf{h}}\} + N^*_{\mathbf{h}}\{\mathbf{P}\cdot\mathbf{M}_{\perp\mathbf{h}}\} + \mathbf{M}_{\perp\mathbf{h}}\cdot\mathbf{M}^*_{\perp\mathbf{h}} + \mathrm{i}\mathbf{P}\cdot\{\mathbf{M}_{\perp\mathbf{h}}\times\mathbf{M}^*_{\perp\mathbf{h}}\} \tag{27}$$

$$\begin{aligned}\mathbf{P}_s I_{\mathbf{h}} = {} & \mathbf{P} N_{\mathbf{h}} N^*_{\mathbf{h}} + N_{\mathbf{h}}\mathbf{M}^*_{\perp\mathbf{h}} + N^*_{\mathbf{h}}\mathbf{M}_{\perp\mathbf{h}} + \mathrm{i}\mathbf{P}\times\{\mathbf{M}_{\perp\mathbf{h}} N^*_{\mathbf{h}} - \mathbf{M}^*_{\perp\mathbf{h}} N_{\mathbf{h}}\} + \mathbf{M}_{\perp\mathbf{h}}\{\mathbf{P}\cdot\mathbf{M}^*_{\perp\mathbf{h}}\} \\ & + \mathbf{M}^*_{\perp\mathbf{h}}\{\mathbf{P}\cdot\mathbf{M}_{\perp\mathbf{h}}\} - \mathbf{P}\{\mathbf{M}_{\perp\mathbf{h}}\cdot\mathbf{M}^*_{\perp\mathbf{h}}\} + \mathrm{i}\{\mathbf{M}_{\perp\mathbf{h}}\times\mathbf{M}^*_{\perp\mathbf{h}}\}\end{aligned} \tag{28}$$

In practical works, for determining magnetic structures it is usual to start with non-polarised neutrons using neutron powder diffraction to determine the propagation vector(s) of the magnetic ordering and treat the intensities to determine the Fourier coefficient that appears directly in equation (24). Powder diffraction, due to the overlap of Bragg reflections, is unable to determine some details of magnetic structures and, many times, appears a situation in which two different magnetic models give exactly the same calculated diffraction pattern. For those cases, only the use of single crystals and polarised neutrons is the appropriate technique for magnetic structure determination.

Formula (27) is the basis for studying *spin densities* induced by an external applied magnetic field thanks to the nuclear–magnetic interference terms, mixing $N_{\mathbf{h}}$ and $\mathbf{M}_{\perp\mathbf{h}}$, appearing in (27). A comprehensive summary of this technique is provided in reference [53] and examples of applications are given in references [54,55]. This technique is able to provide the spatial distribution of unpaired electrons and their departure from spherical shape, which is normally used for magnetic structure determination. For that, very good data of measured flipping ratios are needed. The flipping ratio is defined as: $R = I^+/I^-$, where the superscripts mean the neutron intensity of the scattered beam when the incident neutrons are polarised parallel (+) or anti-parallel (-) to the applied external field.

Formula (28) is the basis of the 3D-*polarimetry* technique [56], in which the sample is maintained at low temperature in strictly zero field, obtained by using the Meissner effect on a special device (CryoPAD, [58]). Using this technique, a full control of the incident and scattered polarisation allows measuring nine components of a matrix (polarisation matrix) related with different components of the magnetic interaction vector. This technique is very precise and allows us to distinguish between chiral domains of helical structures. Examples of the application of this technique can be found in references [57,59], in which 3D polarimetry is used for getting more precise moment directions and magnitudes (CuO, [57]) and for distinguishing different magnetic models ($HoMnO_3$, [59]) giving rise to the same non-polarised neutron diffraction patterns. However, this technique is useless for samples with magnetic structures showing a macroscopic ferromagnetic component due to the depolarisation effects produced by local magnetic fields.

6. Magnetic structures with several propagation vectors

In this section, we will consider some complex cases in which the Fourier series (14) contains several terms corresponding to different propagation vectors that are either in the same star or in different stars. We assume that isotropic exchange interactions are dominant. Anisotropy terms are assumed to be small, and the weak perturbations they introduce (e.g., harmonics) will be ignored. The most powerful experimental technique for the determination of magnetic structures is neutron diffraction. However, in many cases, it does not give a complete information. This can be seen by adding a phase factor, depending only on $\mathbf{k}$, to the Fourier series equation (14):

$$\mathbf{m}_{jl} = \sum_{\{\mathbf{k}\}} \mathbf{S}_{\mathbf{k}j} \exp\{-2\pi\mathrm{i}(\mathbf{k}\mathbf{R}_l + \Psi_{\mathbf{k}})\} \tag{29}$$

The magnetic structure factor [equation (24)] transforms to:

$$\mathbf{M}(\mathbf{H}+\mathbf{k}) = p \exp\{2\pi\mathrm{i}\Psi_{\mathbf{k}}\} \sum_{j=1}^{n_c} f_j(\mathbf{H}+\mathbf{k})\mathbf{S}_{\mathbf{k}j} \exp\{2\pi\mathrm{i}(\mathbf{H}+\mathbf{k})\mathbf{r}_j\} \tag{30}$$

The phase $\Psi_{\mathbf{k}}$ appears in the expression of the magnetic structure factor as a multiplicative phase factor that does not change the intensity of equation (27) or the scattered polarisation of (28) for a pure magnetic reflection. The phases $\Psi_{\mathbf{k}}$ are not accessible experimentally, so the real magnetic structure cannot be obtained from diffraction measurements alone.

The simplest case in which the phase plays an important role is the sinusoidally modulated structure in a simple Bravais lattice (a single magnetic atom per primitive cell) when the propagation vector takes special values. The Fourier coefficient and the corresponding magnetic moment at cell l are:

$$\mathbf{S}_{\mathbf{k}} = \frac{1}{2} m_o \mathbf{u} \exp\{-2\pi\mathrm{i}\Psi_{\mathbf{k}}\} \qquad \mathbf{m}_l = m_o \mathbf{u} \cos 2\pi(\mathbf{k}\mathbf{R}_l + \Psi_{\mathbf{k}})$$

The phase $\Psi_{\mathbf{k}}$ plays no role when $\mathbf{k} \in IBZ$ and has no rational components. Indeed, a change in $\Psi_{\mathbf{k}}$ has the same effect as a change of the origin in the whole crystal. All magnetic moments between $-m_o\mathbf{u}$ and $m_o\mathbf{u}$ are realised somewhere

in the lattice. However, if $\mathbf{k} = p\mathbf{k}/q$, where p/q is a rational number *different from* 0 or 1/2, the phase $\Psi_{\mathbf{k}}$ is relevant. For instance, if $\mathbf{k} = \mathbf{H}/4$ and $\Psi_{\mathbf{k}} = 1/8$ the magnetic structure is a constant moment (CM) structure with the sequence $\{++--++--\ldots\}$. This structure is indistinguishable from the sinusoidally modulated structure obtained with an arbitrary value of $\Psi_{\mathbf{k}}$ like $\{0+0-0+0-\ldots\}$ or $\{S, s, -S, -s, S, s, -S, -s, S, s, -S, -s\ldots\}$. These structures are of course physically different. If all the components of $\mathbf{k}$ are rational, the selection of the phase can have important consequences for the spin arrangement. This is the simplest case in which the physical picture depends on the election of a parameter ($\Psi_{\mathbf{k}}$) that is not accessible by diffraction methods. Physical considerations lead us to prefer one model among several others. For instance, in insulators, in the absence of frustration, CM magnetic structures are normally expected at very low temperatures when magnetic atoms have an intrinsic magnetic moment. This condition reduces the number of ways to combine non-symmetry-related propagation vectors to several specific cases that have been discussed by Nagamiya [60]. Let us discuss some unusual simple cases that will be illustrated with real examples.

6.1. Magnetic structures with several propagation vectors belonging to the same star: multi-**k** structures

The most frequent case of magnetic compounds exhibiting more than one propagation vector is the so-called multi-**k** structures, observed in some intermetallic compounds of high crystallographic symmetry [28]. The term 'multi-**k** structures' refers to a magnetic structure in which more than one arm of the star of **k** participates into the actual spin arrangement. As we will see later, symmetry relations between the Fourier coefficients of the magnetic structure, when all the propagation vectors belong to a single star, can be obtained by representation group theory using the method developed by Bertaut [61] and by Izyumov and collaborators [62].

The usual case is when several propagation vectors of the same star appear in the diffraction pattern. Suppose that we observe magnetic reflections indexed with two propagation vectors, $\mathbf{k}_1 \neq \pm\mathbf{k}_2$, belonging to the same star. Data analysis is generally unable to discriminate between the coexistence of different magnetic domains and a coherent superposition (true multi-**k** structure) of the Fourier coefficients $\mathbf{S}_{\mathbf{k}1}$ and $\mathbf{S}_{\mathbf{k}2}$ in (14). Methods for distinguishing both cases comprise the use of an external magnetic field or uni-axial stress to see if the intensities of satellites change equally or behave differently as a consequence of different domain populations. Examples of multi-**k** structures and the effect of considering multi-**k** in comparison with single-**k** even if the used neutron technique is unable to distinguish between both cases can be found in references [63–65]. The full treatment of multi-**k** structures when the propagation vectors are incommensurable can be done using the superspace formalism (see section 8).

6.2. Magnetic structures with several propagation vectors of different stars: conical structures

The case of two propagation vectors that do not belong to the same star is unusual, except when the spins $\mathbf{S}_{jl}$ of each family j are parallel to the surface of a cone.[4] This corresponds to two propagation vectors $\mathbf{k}_1 = \mathbf{k}$ and $\mathbf{k}_2 = \mathbf{0}$, and Fourier coefficients like in equation (19) for $\mathbf{S}_{\mathbf{k}1}$, and $\mathbf{S}_{\mathbf{k}2} \propto \mathbf{w}$:

$$\mathbf{S}_{jl} = s_j\mathbf{u}_j \sin\alpha_j \cos(2\pi[\mathbf{k}\cdot\mathbf{R}_l + \Psi_j]) + s_j\mathbf{v}_j \sin\alpha_j \sin(2\pi[\mathbf{k}\cdot\mathbf{R}_l + \Psi_j]) + s_j\mathbf{w}_j \cos\alpha_j \tag{31}$$

where α_j and Ψ_j are real parameters and the real unit vectors $\mathbf{u}_j$, $\mathbf{v}_j$, $\mathbf{w}_j$ are orthogonal. Formula (31) is such that $|\mathbf{S}_{jl}|$ is equal to s_j, independently of l as it should be at low temperature, when s_j is the modulus of the spin, which is known (1/2, 1, 3/2, possibly multiplied by the g-factor and the Bohr magneton if we wish to have a magnetic moment rather than a spin). Upon heating, s_j decreases because of thermal fluctuations.

The conical structure (31) can be obtained by applying an external field on a helical spin configuration, or by the interaction of two spin families, one of which is ferromagnetically ordered and the other is helically ordered.

In formula (31) the first two terms correspond to a pair of propagation vectors $\mathbf{k}$ and $-\mathbf{k}$ that may have any position at the *IBZ*, while the last term corresponds to a propagation vector that is 0. Obviously, the pair $\mathbf{k}$, $-\mathbf{k}$ can also be combined with a propagation vector $\mathbf{k}_2 = \mathbf{H}/2$, where $\mathbf{H}$ is a reciprocal lattice vector. Using the notations $\Phi_{\mathbf{k}l} = 2\pi\mathbf{k}\mathbf{R}_l$ and $(-1)^{h_l} = \exp(\pi i\mathbf{H}\cdot\mathbf{R}_l)$, and considering now Ψ_j as multiplied by 2π, the formula (31) should then be replaced by

$$\mathbf{S}_{jl} = s_j\mathbf{u}_j \sin\alpha_j \cos(\Phi_{\mathbf{k}l} + \Psi_j) + s_j\mathbf{v}_j \sin\alpha_j \sin(\Phi_{\mathbf{k}l} + \Psi_j) + s_j\mathbf{w}_j(-1)^{h_l} \cos\alpha_j \tag{32}$$

Nagamiya [60] has shown that $|\mathbf{S}_{jl}|$ can also be independent of l (CM-structures) if $\mathbf{k}_2 = \mathbf{H}/4$, if $\mathbf{k}_2 = -\mathbf{k} + \mathbf{H}/2$, or if $\mathbf{k}_2 = \pm 3\mathbf{k}/2$ for particular orientations of $\mathbf{S}_{\mathbf{k}}$ and $\mathbf{S}_{\mathbf{k}_2}$.

6.3. Two exotic examples

Let us consider exotic cases not verifying Nagamiya's conditions, so the modulus of magnetic moments is varying in the lattice $|\mathbf{S}_{jl}| = f(\mathbf{R}_l)$.

[4] Formula (31) is formula (22.1) of Nagamiya [60].

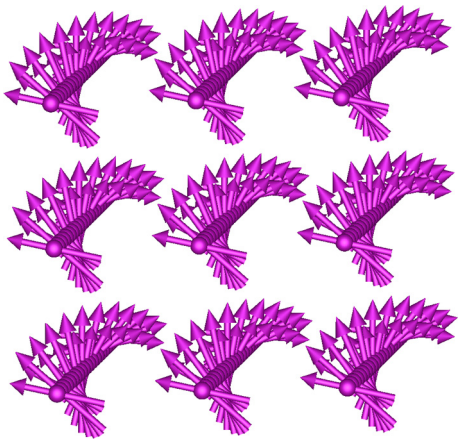

Fig. 7. Magnetic structure of $CsMnF_4$. The modulus of the magnetic moment is not uniform, and longer moments alternate with shorter moments [66].

The compound $CsMnF_4$ [66] apparently combines a pair $(\mathbf{k}, -\mathbf{k})$ of incommensurable propagation vectors, with a propagation vector $\mathbf{H}/2$ that is half a reciprocal lattice vector. The structure is therefore defined by formula (32), but now $\mathbf{w}_j$ is *not* orthogonal to the plane defined by the orthogonal vectors $\mathbf{u}_j$ and $\mathbf{v}_j$. In fact, it is even in that plane. Therefore, the modulus of the magnetic moment is not uniform and depends on l.

$$|\mathbf{S}_{jl}|^2 = s_j^2 + s_j^2 \sin 2\alpha_j (\mathbf{u}_j.\mathbf{w}_j)(-1)^{h_l} \cos(\Phi_{\mathbf{k}l} + \Psi_j) + s_j^2 \sin 2\alpha_j (\mathbf{v}_j \cdot \mathbf{w}_j)(-1)^{h_l} \sin(\Phi_{\mathbf{k}l} + \Psi_j) \tag{33}$$

The modulus $|\mathbf{S}_{jl}|$ varies between the two extreme values $s_j\sqrt{1 - \sin 2\alpha_j \sin\theta}$ and $s_j\sqrt{1 + \sin 2\alpha_j \sin\theta}$, being θ the angle of $\mathbf{w}_j$ with $\mathbf{u}_j \times \mathbf{v}_j$. A schematic picture of the $CsMnF_4$ magnetic structure is shown in Fig. 7.

In addition to the case of $CsMnF_4$, mentioned above, another interesting system is $TbMn_6Ge_6$ [67]. The second wave vector, in this case, is $\mathbf{k} = 0$ and the associated magnetic moment lies within the **u**–**v** plane, defining the spiral plane of the first propagation vector. This gives rise to a distorted cycloidal structure.

In all these cases, an arbitrary phase $\Psi_{\mathbf{q}}$ may be added to the Ψ_j without changing the structure. We shall now consider the case of two pairs of propagation vectors $(\mathbf{k}, -\mathbf{k})$ and $(\mathbf{q}, -\mathbf{q})$ verifying $\mathbf{k}, \mathbf{q} \in IBZ$. Such a magnetic structure has as Fourier coefficients (we drop the index j for simplicity):

$$\mathbf{S}_{\mathbf{k}} = \frac{1}{2}(\mathbf{R}_{\mathbf{k}} + i\mathbf{I}_{\mathbf{k}}) \qquad \mathbf{S}_{\mathbf{q}} = \frac{1}{2}(\mathbf{R}_{\mathbf{q}} + i\mathbf{I}_{\mathbf{q}}) \exp\{-i\Psi\}$$

The magnetic moment distribution is given by:

$$\mathbf{m}_l = \mathbf{R}_{\mathbf{k}} \cos\Phi_{\mathbf{k}l} + \mathbf{I}_{\mathbf{k}} \sin\Phi_{\mathbf{k}l} + \mathbf{R}_{\mathbf{q}} \cos(\Phi_{\mathbf{q}l} + \Psi) + \mathbf{I}_{\mathbf{q}} \sin(\Phi_{\mathbf{q}l} + \Psi) \tag{34}$$

This moment distribution is generally a non-CM structure and the change of the phase factor Ψ can modify the physical picture if both vectors $\mathbf{k}$ and $\mathbf{q}$ have rational components. This last case is interesting when the components are simple integer fractions, because one can treat the problem using the magnetic cell and search for a magnetic space group that fixes automatically the phase. The finding of such a commensurable magnetic structure does not eliminate the problem of uniqueness of the magnetic moment distribution compatible with the experimental results. However, the possibility to have a simple spin arrangement with magnetic moments of atoms approaching the expected intrinsic moment is more satisfying from a physical point of view.

Except for the case of weakly coupled sublattices, the physical origin of the stabilisation of two propagation vectors belonging to different stars is not yet clear in the absence of external fields. In Bravais lattices, we have to think about the action of higher-order terms (biquadratic) in the spin Hamiltonian to stabilise two propagation vectors. In complex crystal structures, the nature of the ground state is not known in the general case and, probably, it is not necessary to invoke higher-order terms to stabilise two non-related propagation vectors. Only the case of conical structures ($\mathbf{k} = 0$ and $\mathbf{q} \in IBZ$) has been studied with some detail [68] for the spinel lattice. We can conclude that only a physical model based on the microscopic spin–spin interactions is able to fix completely the phases appearing in the Fourier expansion of the magnetic moment distribution in the solid. Experimentally, other techniques (like Mössbauer spectroscopy, neutron or X-ray topography, μ-SR, etc.) may help, in some cases, to distinguish between several models. An interesting example, concerned with the application of μ-SR to determine details of the magnetic structure of MnSi/MnGe, can be consulted in [69,70]. Unfortunately, there is no general method allowing us to overcome this *phase problem*. We will see that we can use the invariance symmetry (in the formalism of superspace groups) to select the most symmetric of the possible configurations.

7. Magnetic crystallography. Representations and Shubnikov groups

7.1. Representation analysis for determining magnetic structures

The first person who proposed to use systematically the representation analysis (*RA*) to handle the determination of magnetic structures was E.F. Bertaut [40,61]. Other strong contributors to the method are Y.A. Izyumov and his collaborators. Izyumov published a series of articles [43,62] on *RA* and magnetic structure description and determination, giving explicit and general formulae for deducing the basis functions of the irreducible representations (*irreps*). This is the principal method that has been used in practice up to now for determining magnetic structures. A representation of an abstract group $\mathcal{G}$ is a mapping of the elements of $\mathcal{G}$ to a set of $n \times n$ matrices, $\Gamma = \{\Gamma(g) | g \in \mathcal{G}\}$, which have the same group structure under matrix multiplication. If g_i and g_j are elements of $\mathcal{G}$: $\Gamma(g_i)\Gamma(g_j) = \Gamma(g_i \circ g_j)$, where $\Gamma(g)$ is the matrix corresponding to the element g. The number n is the dimension of the abstract *representation space* in which the matrices are embedded and is called the *dimension* of the representation. Whatever group has an infinite number of representations. Two representations are equivalent if there is a similarity transformation between them common two all matrices: $\Gamma'(g) = U\Gamma(g)U^{-1}$. If we are able to find an appropriate U-matrix that reduces the matrix-set of the representation to a block-diagonal form, the individual sub-matrices are also representations of the group. We say that the original representation is decomposed in the direct sum of smaller representations and we write symbolically:

$$\Gamma = \sum_{\oplus \nu} n_\nu \Gamma^\nu = n_1\Gamma^1 \oplus n_2\Gamma^2 \oplus \ldots \oplus n_m\Gamma^m \tag{35}$$

If the dimensions of representations Γ^ν are the smallest possible, the sub-matrices for the different group elements are called *irreducible representations* (*irreps*) and they play an important role in group theory (see, for instance, [71]). The so-called *basis functions* of the *irreps* [40,41,43] correspond to vectors (similar to *normal modes* in lattice vibration theory) spanning a working functional space that can be calculated using mathematical techniques (*projection operators*) of group theory. There are few crucial theorems and concepts concerning representations that can be found in section 4 of reference [41] and we will not repeat them here.

Proper crystal structures (disregarding quasi-crystals and modulated structures) have symmetries that are described using one of the 230 space groups.[5] The elements of these groups are constituted by operators of the form $\hat{g} = \{g|\mathbf{t}\}$ (in Seitz notation), where g represents the so-called *rotational part* and $\mathbf{t}$ is a translation. The rotational operators g are normally described as 3×3 matrices operating in the Euclidean 3D space referred to the basis given by the vectors $\mathbf{a}_i$; the translation part of the operator is written as $\mathbf{t} = t_1\mathbf{a}_1 + t_2\mathbf{a}_2 + t_3\mathbf{a}_3$. The possible rotations are limited and can be easily obtained from the fact that the trace of the matrices representing rotations is an invariant independent of the selected frame and they have to leave invariant the direct lattice L^d. The equation limiting the possible rotations of angle θ is: $2\cos\theta \pm 1 \in \mathbb{Z}$, the solutions are: $\theta = n\pi/4$ or $n\pi/6$ with $n \in \mathbb{Z}$. There is a special operator, satisfying always the equation for a lattice, called *space inversion* that, which acts over positions changing the sign of all coordinates. It is represented generally by the symbol $\overline{1} = \{-1|\mathbf{t}\}$. When combined with a rotation, the resulting operator contains a rotational part called an improper rotation (or *rotoinversion*). In general, a proper rotation is represented by a matrix with determinant $\det(g) = 1$. We call improper rotations those with $\det(g) = -1$. When combined with some kind of translation, we have operators representing *screw* or *glide* motions. The action of the operator $\hat{g}$ on vector positions (or polar vectors) is $\{g|\mathbf{t}\}\mathbf{r} = g\mathbf{r} + \mathbf{t}$. The elements for which $\mathbf{t}$ is a lattice translation ($\mathbf{t} \in L^d$) and g is the identity (denoted 1) form a normal subgroup (all its operators commute with those of the group $\mathcal{G}$) called the translation group $\mathcal{T} = \{\{1|\mathbf{t}\} | \mathbf{t} \in L^d\}$. The groups for which an appropriate selection of the origin makes possible to have only elements of the form $\{g|\mathbf{t}\}$ with $\mathbf{t} \in L^d$, are called *symmorphic*. For the *non-symmorphic* groups, there are elements of the form: $\{g|\mathbf{t}\}$, with $t_i \in \mathcal{Q}$ (rational numbers) and they represent screw rotations or glide planes depending on whether the rotation part g is proper or improper, respectively. The presence (or absence) of the space inversion in the symmetry group of a crystal structure determines the absence (presence) of important macroscopic physical properties (piezo-electricity, ferro-electricity, etc.).

If the atoms have magnetic moments, how do they behave under these transformations? A magnetic moment has a part that is related to the orbital angular momentum $\mathbf{L}$, and a part that is related to the spin angular momentum $\mathbf{S}$. We shall only discuss (within classical mechanics) the transformation rules of the orbital angular momentum and assume they are the same for the spin. The effect of a proper rotation $\hat{g} = \{g|0\}$ on an orbital angular momentum $\mathbf{L}$ is to transform it into $g\mathbf{L}$. The space inversion conserves the orbital moment $\mu\mathbf{r} \times \dot{\mathbf{r}}$ of a particle of mass μ at $\mathbf{r}$ because $\mathbf{r} \to -\mathbf{r}$ and $\dot{\mathbf{r}} \to -\dot{\mathbf{r}}$. A translation of vector $\mathbf{t}$ also conserves the average orbital moment because $\mathbf{t} \times \dot{\mathbf{r}}$ averages to 0 for an electron that rotates around a fixed nucleus. The magnetic moment (combination of $\mathbf{L}$ and $\mathbf{S}$) is then an *axial* vector (the cross-product

[5] The determination of the 230 crystallographic space groups was performed at the end of the nineteenth century independently by Fedorov and by Schoenflies. Independently? It is not exactly the right word, as seen from the story of the discovery told by Shafranovskii and Belov. (It can be found in a biography of Fedorov, available through Internet.) In 1888 Fedorov and Schoenflies discovered that they were pursuing the same goal. Then the two scientists exchanged many letters as the number of space groups raised to 227, then 228 and finally 230. Nowadays, scientists do not care about the lengthy derivations (Schoenflies' book [72] has more than 600 pages) and are contented with the catalogue of the 230 space groups [73]. Moreover, there are computing programs for working with space groups in a straightforward manner.

$\mathbf{r} \times \dot{\mathbf{r}}$ is responsible for that). So, in general, the action of the operator $\hat{g}$ on the axial vectors attached to a position $\mathbf{r}$ (like magnetic moments) is a new axial vector $\hat{g}\mathbf{m} = \det(g) g\mathbf{m}$ at the position $g\mathbf{r} + \mathbf{t}$, where $\det(g)$ is the determinant of the matrix representing the rotational part of $\hat{g}$. As a consequence, the action of space inversion on a magnetic moment leaves it invariant: $\overline{1}\mathbf{m} = (-1)(-\mathbf{m}) = \mathbf{m}$.

A space group has an infinite number of elements; however, the presence of the normal translation group allows its decomposition in cosets whose number is always finite: $\mathcal{G} = 1\mathcal{T} + \hat{g}_2\mathcal{T} \ldots + \hat{g}_n\mathcal{T}$. The number n is denoted by $|\mathcal{G}|$, and corresponds to the order of the factor group with respect to the $\mathcal{T}$ group. In the International Tables of Crystallography [73], the coset representatives of each space group are tabulated using the so-called Jones faithful symbols. The number $|\mathcal{G}|$ is called *general multiplicity* of the space group. For instance, the operator $\hat{g} : -x, -y, -z$ represents an inversion centre at the origin; the operator $\hat{g} : x + 1/2, -y, -z$ represents a screw twofold rotation along the $\mathbf{a}_1$ axis. Notice that the Jones faithful symbols may also be interpreted as positions in 3D Euclidean space.

The important facts that we want to stress in this paragraph, concerned with representations of space groups, are the following.

1. Magnetic ordering occurs below a certain temperature as a phase transition and the order parameters can be described by the phenomenological Landau theory taking into account the *irreps* of the space group $\mathcal{G}$ of the crystal in the paramagnetic state. The so-called *magnetic representation*, Γ_{mag}, is a set of matrices of dimension $3n_{aj} \times 3n_{aj}$, n_{aj} being the number of magnetic atoms corresponding to the site j generated by the symmetry operators of $\mathcal{G}$ acting on the set of n_{aj} complex Fourier coefficients. This representation is easily obtained as the direct product of an axial 3D-representation (matrices of the action of $\hat{g}$ on magnetic moments) and a *permutation* representation exchanging the n_{aj} atoms in the unit cell. If the propagation vector is different from zero, one has to consider the group of $\mathbf{k}$ (see next item).
2. The *irreps* of $\mathcal{G}$ can be calculated (or obtained from tables) from the *irreps* of the propagation vector group $\mathcal{G}_{\mathbf{k}} = \{\hat{g} \in \mathcal{G} | \mathbf{k}g^{-1} = \mathbf{k} + \mathbf{H}, \mathbf{H} \in L^*\}$ (subgroup of $\mathcal{G}$ constituted by the elements of $\mathcal{G}$ leaving invariant the $\mathbf{k}$-vector). The *irreps* of $\mathcal{G}_{\mathbf{k}}$ are called *small* representations. The set of $\mathbf{k}$-vectors, $\{\mathbf{k}\}$, generated by the application of all the rotational symmetry element of $\mathcal{G}$ is called the *star* of the propagation vector. The *irreps* of $\mathcal{G}$ are characterised by the full *star* $\{\mathbf{k}\}$ and are obtained from the *irreps* of $\mathcal{G}_{\mathbf{k}}$ by applying the *induction formula* (see formula (30) of [41]).
3. The possible magnetic configurations are related to the *irreps* of the paramagnetic space group in such a way that the Fourier coefficients $\mathbf{S}_{\mathbf{k}j}$ are linear combinations of the *irreps* basis functions (vectors in the present case). The basis vectors of the *irreps* are obtained using the projector operator formula (see the full section 7 of [41]). For obtaining the so-called atomic components of the basis function, we can use formula (54) of [41]. For a magnetic site j that has equivalent positions $js (s = 1, 2, \ldots, n_{aj})$ (orbit of j: $\mathbf{r}_{js} = \{g|\mathbf{t}\}_s \mathbf{r}_{j1}$, generated by the symmetry operators of the propagation vector group including the operations transforming $\mathbf{k}$ into $-\mathbf{k}$), the Fourier coefficients can be written as:

$$\mathbf{S}_{\mathbf{k}js} = \sum_{n\lambda} C^{\mathbf{k}\nu}_{n\lambda} \mathbf{S}^{\mathbf{k}\nu}_{n\lambda}(js) \tag{36}$$

where ν labels the active *irrep* Γ^ν of $\mathcal{G}_{\mathbf{k}}$ and λ the component corresponding to the dimension of the *irrep* ($\lambda = 1, 2, \ldots \dim(\Gamma^\nu)$); here the index n varies between one and the number of times Γ^ν is contained in the global magnetic representation Γ_{mag} (see Eq. (35)). The constant vectors $\mathbf{S}^{\mathbf{k}\nu}_{n\lambda}(js)$ are the atomic components of the *irreps* basis functions and can be calculated by hand or using computing programs. The coefficients $C^{\mathbf{k}\nu}_{n\lambda}$, called *mixing coefficients* by Izyumov [62], are now the free parameters of the magnetic structure and have to be determined experimentally. The number of such coefficients is generally lower than the total number of Fourier components without considering symmetry.

In expression (24), the atoms are assumed to be at rest. If thermal motion, through isotropic temperature factors, is considered and if symmetry analysis is established for coupling the different Fourier components (using Eq. (36)), we obtain the general expression of the magnetic structure factor for $\mathbf{h} = \mathbf{H} + \mathbf{k}$:

$$\mathbf{M}(\mathbf{h}) = p \sum_{js} f_j(h)\, \mathrm{e}^{-B_j|h/2|^2} \mathbf{S}_{\mathbf{k}js} \exp\{2\pi \mathrm{i} \mathbf{h}\mathbf{r}_{js}\} \tag{37}$$

$$\mathbf{M}(\mathbf{h}) = p \sum_{j} f_j(h)\, \mathrm{e}^{-B_j|h/2|^2} \sum_{n\lambda} C^{\mathbf{k}\nu}_{n\lambda} \sum_{s} \mathbf{S}^{\mathbf{k}\nu}_{n\lambda}(js) \exp\{2\pi \mathrm{i} \mathbf{h}\mathbf{r}_{js}\} \tag{38}$$

The determination of magnetic structures using *RA* is reduced to find the coefficients $C^{\mathbf{k}\nu}_{n\lambda}$ comparing the measured magnetic Bragg intensities with the calculated ones using the expressions ((26), (25), (38) or (27) and (28)), depending on the neutron scattering technique to be used.

7.2. Magnetic space groups: Shubnikov groups

The *RA* provides a method for reducing the number of free parameters for describing a magnetic structure that takes place in a crystal with structure belonging to one of the 230 space groups. However, the symmetry invariance (*SI*) of the

particular spin configuration is not tackled by the representation method. For doing that, the theory of magnetic space groups is the adequate one for commensurable structures. The general Hamiltonian given by Eq. (12) is obviously invariant for all the symmetry operators of the space group – in the case of pure Heisenberg Hamiltonian (Eq. (13)), whatever rotation of all moments leaves it invariant. Moreover, the Hamiltonian dependency on even powers of spins makes that it is invariant with respect to the time reversal. This corresponds (it is obvious for the orbital part, which is linear on $\mathrm{d}/\mathrm{d}t$) to the sign change of all spins. This is the basis for introducing a new symmetry operator, denoted $1'$ (or $\{1'|0\}$), called *time reversal* or *spin reversal* that acts only on magnetic moments as: $1'\mathbf{m} = -\mathbf{m}$. If we combine a symmetry operator $\hat{g}$ with $1'$, we simply write $\hat{g}'$ (a *primed* element). Now a general operator $\hat{g}$ acts on magnetic moments as: $\hat{g}\mathbf{m} = \delta \det(g) g\mathbf{m}$, where δ is the *signature* of the operator, that is, $\delta = 1$ if the operator is *not primed* and $\delta = -1$ if the operator is *primed*. In Seitz-like notation, one can write a general symmetry operator as $\hat{g} = \{g, \delta|\mathbf{t}\}$. Taking the direct product of the time-reversal group, $\mathcal{R} = \{1, 1'\}$ with the 230 space group, we obtain the so-called 230 *grey groups* or *paramagnetic groups*. These groups can only describe paramagnetic ordering because the operator $\{1'|0\}$ is always present and the only solution to the equation $1'\mathbf{m} = \mathbf{m}$ for an atom at whatever position is $\mathbf{m} = 0$. The notation used for paramagnetic groups is the same (Hermann–Mauguin) as that for crystallographic groups, followed by the symbol $1'$. For instance, the paramagnetic group of many transition metal perovskites crystallising in the space group $Pbnm$ is $Pbnm1'$. The magnetic groups allowing a configuration with non-null moments cannot contain $\{1'|0\}$ as an independent operator and are, in fact, subgroups of the *paramagnetic* groups. The operators of the form $\{1'|\mathbf{n}\}$, in which $\mathbf{n}$ is a lattice translation, constitute the so-called *anti-translations*. Notice that, in the section concerned with representations, we have not used the time reversal symmetry (primed operators) at all. The concept of propagation vector(s) in the Fourier series (14) replaces to some extent the anti-translations in describing commensurable magnetic structures having $\mathbf{k} = \mathbf{H}/2$.

Let us summarise the history of magnetic groups and the role they played up to now. In 1945, Shubnikov re-introduced the time-reversal group $\mathcal{R} = \{1, 1'\}$, first described by Heesch in 1929 [74]; then, in 1951, Shubnikov described the bi-colour point groups.[6] In 1955, Belov, Neronova, and Smirnova provided for the first time the full list of the 1651 magnetic space groups (or *Shubnikov* groups) [75]. In 1957, Zamorzaev derived, using group theory, the Shubnikov groups [76].[7] In 1965, Opechowski and Guccione derived the list of Shubnikov groups by a method that "satisfies the requirements of mathematical rigour" [77]. The whole set of Shubnikov groups was deduced from the subgroups of index 2 of the space groups. The origin of this fact is that the product of two primed elements is a non-primed element, so the structure of these groups is such as half the coset representatives are primed. Opechowski started a polemic with Bertaut (promoting *RA*) about the advantages of describing magnetic structures using Shubnikov groups (Opechowski). In 1968, Bertaut summarised the description of magnetic structures based on *RA* [40] and stated that *RA* was *superior* to the *SI* method of Shubnikov groups, mostly because it can handle whatever **k**-vector inside the Brillouin zone (e.g., incommensurate structures); however, he stated that Shubnikov groups are still useful for describing the physical properties of magnetic systems.[8] During the same year, 1968, a new book, *Describing 3-dimensional Periodic Magnetic Structures by Shubnikov Groups*, was published, relating Shubnikov groups to magnetic structures [78].

The *RA* method was dominating the field of magnetic structure determination thanks to the influence of the Grenoble school and the leadership of Erwin Félix Bertaut. Moreover, the published works on magnetic space groups were not complete and the equivalent of the Wyckoff positions in crystallographic groups were never described; two kinds of notations (OG for Opechowski–Guccione and BNS for Belov–Neronova–Smirnova) were used by different authors. It was only in 2001 that Daniel B. Litvin provided for the first time a full description of all Shubnikov groups in an electronic book, freely accessible, similar to the International Tables, but too big to be printed on paper [79]. Only in 2010, the data provided by D.B. Litvin were put available in a database compiled by H.T. Stokes and B.J. Campbell [80], in which both notations OG and BNS were used.

Finally, the magnetic space groups can be classified into four types.

1. Type 1, or *monochrome* groups, corresponding to the 230 crystallographic group: $\mathcal{M} = \mathcal{G}$. No primed operators exist in these groups.
2. Type 2, or *grey* groups or *paramagnetic* groups, corresponding to the 230 crystallographic groups plus the product of time reversal by all operators of the group: $\mathcal{M} = \mathcal{G} + \mathcal{G}1'$. These groups have as much as the double number of operators of the corresponding crystallographic group. The notation of these groups is exactly the conventional Hermann–Mauguin symbol followed by the symbol $1'$. A crystal invariant by such a group cannot be magnetically ordered.
3. Type 3, or black and white of first species (BW1); they are constructed from an equi-translational subgroup $\mathcal{H}$ of index 2 of the parent crystallographic group $\mathcal{G}$, so that $\mathcal{M} = \mathcal{H} + (\mathcal{G} - \mathcal{H})1'$. These groups have exactly half of their operators that are *primed*. Their corresponding point group (determining the macroscopic physical properties) is a *coloured* group. The notation of these groups is the same as the Hermann–Mauguin symbol of $\mathcal{G}$, except

[6] A point group is a finite group whose elements are proper and improper rotations of a space group. They can be obtained from the space group suppressing all translations and conserving only the rotational part of the operators $\hat{g}$.

[7] In the above-mentioned works, the authors did not care about magnetic structures. Their concern was purely the mathematical properties of this kind of groups and how to classify them. Some authors use the term Shubnikov/Heesch groups.

[8] In paragraph 7 of [40], it is said: *Can we ignore magnetic groups entirely? The answer is no, not only in microscopic, say atomic systems… but also macroscopically when a magnetic system is coupled with other forms of energy*.

that the appropriate generators are primed, e.g., if $\mathcal{G} = Pnna$, one can have the following Shubnikov groups $\mathcal{M}$: $Pn'na$, $Pnn'a$, $Pnna'$, $Pn'n'a$, $Pn'na'$, $Pnn'a'$, $Pn'n'a'$. These groups, including the *monochrome* $Pnna$, correspond to the eight 1D *irreps* of $Pnna$ for $\mathbf{k} = 0$. There are 674 BW1 groups.

4. Type 4, or black and white of second species (BW2); they are constructed from an equi-class subgroup $\mathcal{H}$ of index 2, of the parent crystallographic group. As for type 3, $\mathcal{M} = \mathcal{H} + (\mathcal{G} - \mathcal{H})1'$, but now half of the original translations are *primed*: these groups have then a *coloured* lattice. The notation used for these groups can be based in the subgroup $\mathcal{H}$ (BNS notation) or in the parent crystallographic group $\mathcal{G}$ (OG notation). This occurs only for this type of magnetic groups; for all the other groups, the BNS and OG notations coincide. In both cases, the first symbol indicates the kind of coloured lattice even if they differ for both notation. In the BNS notation, the lattice symbol indicates the anti-centring vector(s) and none of the generators constituting the symbol are primed. It is assumed that the groups are referred to the *magnetic unit cell* (the unit cell of $\mathcal{H}$). This is not the case of the OG notation, in which the operators are referred to the conventional crystallographic cell of the $\mathcal{G}$ group. As an example, the magnetic group number 417 has as BNS notation P_Cnna and OG notation $C_Pcc'a'$. In the BNS convention this group belongs to the family of $Pnna$ whereas for the OG convention it belongs to the family of the group $Ccca$. There are 517 BW2 groups.

The total number of Shubnikov groups is 1651, corresponding to the sum of the different types: $230 + 230 + 674 + 517$. The expression of the magnetic structure factor when using the BNS formulation is given in terms of the real magnetic moments and can be written generally as:

$$\mathbf{M}(\mathbf{h}) = p \sum_{j=1}^{m_a} O_j f_j(h)\, e^{-B_j|h/2|^2} \sum_{s=1}^{|\mathcal{M}|} \hat{g}_s \mathbf{m}_j \exp\{2\pi i \mathbf{h} \hat{g}_s \mathbf{r}_j\} \tag{39}$$

$$\mathbf{M}(\mathbf{h}) = p \sum_{j=1}^{m_a} O_j f_j(h)\, e^{-B_j|h/2|^2} \sum_{s=1}^{|\mathcal{M}|} \delta_s \det(g_s) g_s \mathbf{m}_j \exp\{2\pi i \mathbf{h}[g_s \mathbf{r}_j + \mathbf{t}_s]\} \tag{40}$$

where p is defined below formula (20), m_a is the number of magnetic atoms in the asymmetric unit of the Shubnikov group, $|\mathcal{M}|$ is the general multiplicity of the group and $O_j = m_j/|\mathcal{M}|$ is an occupation factor that takes into account the fact that it may be magnetic atoms in special positions of multiplicity m_j.

Nowadays there are resources on the internet and computing programs that allow one to consult the complete list of the magnetic space groups, their special (Wyckoff) positions, and the corresponding conditions to be verified by the magnetic moments. We will see an analysis of the current resources in section 9.

8. Superspace approach to invariance symmetry of crystal structures and spin configurations

8.1. Concept of superspace

The basic concepts related with incommensurate crystal structures and their symmetry description using superspace groups can be found in references [81–87]. The case of magnetic superspace groups has been treated exhaustively in reference [88] and here we will follow some of their explanations and generalise some expressions for multiple propagation vectors.

The concept of superspace comes from the consideration that all Bragg spots observed in a modulated structure can be indexed using a series of modulation (propagation) vectors $\mathbf{q}_p$ with $p = 1, 2, \ldots, d$. The scattering vector for a Bragg spot (diffraction vector) can be written as:

$$\mathbf{h} = h_1 \mathbf{a}_1^* + h_2 \mathbf{a}_2^* + h_3 \mathbf{a}_3^* + \sum_{p=1}^{d} m_p \mathbf{q}_p \tag{41}$$

The extra integer indices m_p correspond to the harmonics of the modulation vector $\mathbf{q}_p = \sigma_{1p}\mathbf{a}_1^* + \sigma_{2p}\mathbf{a}_2^* + \sigma_{3p}\mathbf{a}_3^*$ and there are generally small integers. Even if the modulation vectors are referred to the reciprocal lattice of the real 3D space, one can consider the indices $(h_1, h_2, h_3, m_1, \ldots, m_d)$ or $\mathbf{H}_S = (h_1, h_2, h_3, h_4, \ldots, h_{3+d})$ as the nodes of a $(3+d)$D reciprocal lattice of a superspace that *intersects* the 3D physical space (called also *external* space, V_E). The spots in the 3D reciprocal space, described by Eq. (41), are obtained by orthogonal *projection* of the $(3+d)$D reciprocal lattice onto the 3D reciprocal space. The vectors in the superspace have $3+d$ components and can be written in the form $\mathbf{v}_S = (\mathbf{v}_E, \mathbf{v}_I)$, in which the first vector refers to the 3D external space and the second one to the so-called *internal space*, V_I, and has d components. The superspace V_S is the direct sum of two orthogonal subspaces: the external and the internal spaces $V_S = V_E \oplus V_I$.

The discussion about the basis of the superspace and the geometrical interpretation of the different terms can be consulted in reference [87]. Let us state only that the basis vectors generating the reciprocal and the direct $(3+d)$D lattices are given by:

$$\mathbf{a}_{Si}^* = (\mathbf{a}_i^*, \mathbf{0}) = \mathbf{a}_i^* \quad i = 1, 2, 3 \qquad \mathbf{a}_{S(3+p)}^* = (\mathbf{q}_p, \mathbf{e}_p^*) = \mathbf{q}_p + \mathbf{e}_p^* \quad p = 1, 2, \ldots, d \tag{42}$$

where the $\mathbf{e}_p^*$ are orthogonal to the V_E space. The reciprocal basis to (42), verifying $\mathbf{a}_{Sp}\cdot\mathbf{a}_{Sq}^* = \delta_{pq}$, is given by the equations:

$$\mathbf{a}_{Si} = (\mathbf{a}_i, -\sum_{p=1}^{d}(\mathbf{q}_p\cdot\mathbf{a}_i)\mathbf{e}_p) = \mathbf{a}_i - \sum_{p=1}^{d}(\mathbf{q}_p\cdot\mathbf{a}_i)\mathbf{e}_p \quad i=1,2,3 \qquad \mathbf{a}_{S(3+p)} = (\mathbf{0},\mathbf{e}_p) = \mathbf{e}_p \quad p=1,2,\ldots,d \tag{43}$$

where $\mathbf{e}_p$ are unitary vectors perpendicular to the physical space, ensuring that the embedding of the 3D physical space in the $(3+d)$D space takes place by an orthogonal projection of the reciprocal $(3+d)$D lattice into the physical space or the intersection of the direct 3D space with the $(3+d)$D superspace (see [84,87] for details).

Notice that the scattering vector (42) referred to the reciprocal lattice of the superspace can be written as:

$$\mathbf{H}_\mathrm{S} = h_1\mathbf{a}_{S1}^* + h_2\mathbf{a}_{S2}^* + h_3\mathbf{a}_{S3}^* + \ldots h_{3+d}\mathbf{a}_{S(3+d)}^* \tag{44}$$

The integer indices $(h_1,h_2,\ldots,h_{3+d})$ in (44) are identical to $(h_1,h_2,\ldots,m_1,\ldots,m_d)$ in (42), but the vectors $\mathbf{h}$ and $\mathbf{H}_\mathrm{S}$ are referred to different bases.

8.2. Atomic positions, basic structure and modulation functions

In an ordinary crystal structure, the position of an atom in the crystal is given by (see section 3.3): $\bar{\mathbf{r}}_{jl} = \mathbf{R}_l + \bar{\mathbf{r}}_j$. All the atoms j are translationally equivalent. We have changed the notation adding a bar on top of the vector position to indicate that, in a modulated structure, this represents an *average* or *basic* 3D periodic structure. In a real modulated incommensurate structure, there is no translational symmetry in 3D. The atom position of the atom j in the crystal is given by $\mathbf{r}_{jl} = \bar{\mathbf{r}}_{jl} + \mathbf{u}_j(\mathbf{q}_1\bar{\mathbf{r}}_{jl},\ldots\mathbf{q}_d\bar{\mathbf{r}}_{jl})$, where the modulation functions $\mathbf{u}_j(\mathbf{q}_1\bar{\mathbf{r}}_{jl},\ldots\mathbf{q}_d\bar{\mathbf{r}}_{jl})$ are defined for the atoms within a unit cell of the basic structure and are periodic of period 1 in whatever of its arguments $\mathbf{q}_p\bar{\mathbf{r}}_{jl}$. Notice that we are considering only the ordinary 3D space in these definitions. The modulation functions are displacement polar vectors, referred to the 3D basis of the average structure, depending only on a series of d extra coordinates that can be considered as belonging to the internal space V_I of the superspace. These coordinates are related to the modulation vectors and the atom positions of the basic structure according to the following definitions:

$$\bar{x}_\alpha = (\bar{\mathbf{r}}_{jl})_\alpha \quad \alpha=1,2,3 \tag{45}$$

$$\bar{x}_{3+p} = t_p + \mathbf{q}_p\bar{\mathbf{r}}_{jl} = t_p + \mathbf{q}_p(\mathbf{R}_l+\bar{\mathbf{r}}_j) = t_p + \sigma_{1p}\bar{x}_1 + \sigma_{2p}\bar{x}_2 + \sigma_{3p}\bar{x}_3 \quad p=1,2,\ldots,d \tag{46}$$

where t_p are initial phases of the different waves that concern only the internal space. As it is usual in the literature of superspace, we have dropped the indices j, l from the coordinates, so it is understood that for the coordinate numbered p, we have: $\bar{x}_p = \bar{x}_p(j,l)$. Sometimes, we will explicit the dependency on the atom j with a superscript on modulation functions or parenthesis in coordinates e.g., $\bar{x}_p(j)$, or $\bar{x}_p^j$. In fact, the variables $\bar{x}_p$ can be considered as continuous, so that, depending on the context, they are evaluated for particular points like $\bar{x}_p = t_p + \mathbf{q}_p\bar{\mathbf{r}}_{jl}$.

The most general expression for the modulation functions can be written as a general real Fourier series:

$$\mathbf{u}_j(\bar{x}_4,\bar{x}_5,\ldots,\bar{x}_{3+d}) = \sum_{n_1=0}^{\infty}\ldots\sum_{n_d=0}^{\infty}\mathbf{A}_j^{(n_1,\ldots,n_d)}\cos[2\pi(n_1\bar{x}_4+\ldots+n_d\bar{x}_{3+d})] + \mathbf{B}_j^{(n_1,\ldots,n_d)}\sin[2\pi(n_1\bar{x}_4+\ldots+n_d\bar{x}_{3+d})] \tag{47}$$

The 3D vectorial functions $\mathbf{u}_j$ are different for each atom $j=1,\ldots,n_a$ within the unit cell of the basic structure, and depend on d continuous variables $\bar{x}_p$. If one wants to evaluate the displacement of atom j in the unit cell l in physical space, the continuous arguments should be replaced by the expressions (46). This series takes into account the possibility of having mixed terms that are more general that the superposition of individual waves, of the form $\mathbf{u}_j(\bar{x}_{3+p})$, depending only on one modulation vector. The modulation functions, defined by Eq. (47), verify that they are periodic of period 1 in each of the internal coordinates: $\mathbf{u}_j(\ldots,\bar{x}_{3+p}+1,\ldots) = \mathbf{u}_j(\ldots,\bar{x}_{3+p},\ldots)$, so the argument of the modulation functions can be restricted to real numbers modulo 1. The argument of a modulation function is then a vector of the internal part of the superspace, so we can write $\mathbf{u}(\bar{x}_4,\bar{x}_5,\ldots,\bar{x}_{3+d}) = \mathbf{u}(\bar{\mathbf{r}}_\mathrm{I})$. For magnetic moments $\mathbf{m}_j(\bar{x}_4,\bar{x}_5,\ldots,\bar{x}_{3+d})$, we can also use an expression similar to (47), the only difference being that magnetic moments are axial vectors and behave differently than polar vectors under symmetry operations.

The embedding of the 3D crystal structure in the superspace coordinates for the atom j is done by assuming that the *average* structure is described by the fractional coordinates $\bar{x}_{S\alpha}^j = \bar{x}_\alpha(j)$ $(\alpha=1,2,\ldots,3+d)$ with respect to the basis (43). The positions of an atom j in superspace is a continuous function [81] (wavy line for $d=1$, a hypersurface in general) within the unit cell of the superspace described by the coordinates:

$$x_{S\alpha}^j = \bar{x}_{S\alpha}(j) + u_{j\alpha}(\bar{x}_4,\bar{x}_5,\ldots,\bar{x}_{3+d}) \quad \alpha=1,2,3 \tag{48}$$

$$x_{S(3+p)}^j = \bar{x}_{S(3+p)}(j) + \mathbf{q}_p\mathbf{u}_j(\bar{x}_4,\bar{x}_5,\ldots,\bar{x}_{3+d}) \quad p=1,2,\ldots,d \tag{49}$$

These coordinates constitute a vector in superspace that can be written as:

$$\mathbf{r}_S^j = (x_{S1}^j, x_{S2}^j, \ldots x_{S(3+d)}^j) = (\mathbf{r}_E^j, \mathbf{r}_I^j) \tag{50}$$

With these definitions, one can extend, by analogy with the 3D case, the nuclear scattering density and magnetisation density to the superspace, so that its intersection with physical space gives the 3D densities:

$$\rho_S(\mathbf{r}_S) = \frac{1}{V}\sum_{\mathbf{H}_S} F(\mathbf{H}_S)\exp[-2\pi i \mathbf{H}_S\mathbf{r}_S] \tag{51}$$

$$\mathbf{m}_S(\mathbf{r}_S) = \frac{1}{V}\sum_{\mathbf{H}_S} \mathbf{M}(\mathbf{H}_S)\exp[-2\pi i \mathbf{H}_S\mathbf{r}_S] \tag{52}$$

where the coordinates of $\mathbf{H}_S$ are referred to the reciprocal lattice of the superspace (Eq. (42)) and the coordinates of $\mathbf{r}_S$ are referred to the direct lattice of the superspace (Eq. (43)). For the relations between the density in physical (external) space and that in superspace, the reader is referred to reference [87]. For a short description of the extension to superspace of scalar, vector, and tensor physical properties attached to atoms, see reference [89].

For incommensurate magnetic structures, the description of moment distribution has been discussed in section 4. Here we will use the adequate notation for treating invariance symmetry in the framework of superspace. We will concentrate on the simple case having a single propagation vector ($d = 1$, pair $\mathbf{k}$, $-\mathbf{k}$), so a single additional coordinate $\bar{x}_4 = \tau + \mathbf{k}\bar{\mathbf{r}}_{jl}$. The Fourier series (14) is written here as:

$$\mathbf{m}_{jl} = \mathbf{m}_j(\bar{x}_4) = \sum_{n=-m}^{m} \mathbf{T}_{\mathbf{k}j}^{(n)} \exp(-2\pi i n\mathbf{k}\cdot(\mathbf{R}_l + \mathbf{r}_j)) = \sum_{n=0}^{m}[\mathbf{M}_{cj}^{(n)}\cos(2\pi n\bar{x}_4) + \mathbf{M}_{sj}^{(n)}\sin(2\pi n\bar{x}_4)] \tag{53}$$

where implicitly the term $n = 0$ corresponds to a zero propagation vector and the other terms correspond to the incommensurate magnetic structure. The notation $\mathbf{m}_j(\bar{x}_4)$ indicates that the distribution of magnetic moments in the crystal can be considered directly as modulation functions. The cosine $\mathbf{M}_{cj}^{(n)}$ and sine $\mathbf{M}_{sj}^{(n)}$ amplitudes are related to the real and imaginary components of the Fourier component $\mathbf{S}_{\mathbf{k}j}^{(n)}$ (17) because $\mathbf{S}_{\mathbf{k}j}^{(n)} = \mathbf{T}_{\mathbf{k}j}^{(n)}\exp[-2\pi i n\mathbf{k}\cdot\mathbf{r}_j]$.

In order to take into account the invariance symmetry of a modulated, crystallographic or magnetic, incommensurate structure, let us consider applying a Shubnikov operator to the actual 3D structure. This will transform it into another incommensurate structure that has the same average structure. So they differ only in the modulation functions; a common phase shift in the internal coordinates may recover the original structure. A symmetry operator $\hat{g} = \{g, \delta|\mathbf{t}\}$ of the average structure can be *extended* with a translation in the internal coordinate $\bar{x}_4$. One can then define an operator in 3D space as $\hat{g} = \{g, \delta|\mathbf{t}, \tau\}$, that is, a symmetry operator if it leaves invariant the whole structure. In 3D, a symmetry operator acts on the propagation vector as $\hat{g}\mathbf{k} \rightarrow \mathbf{k}g = \epsilon_g\mathbf{k} + \mathbf{h}_g$, where ϵ_g is equal to 1 or -1 and $\mathbf{h}_g$ is a reciprocal lattice vector that depends on the operator $\hat{g}$. This is a compatibility condition that a symmetry operator of the basic structure has to satisfy for being promoted as a superspace symmetry operator.

8.3. Form of operators in superspace

It is possible to work with *extended* operators, just considering phase factors in the internal space; however, one can define a general operator in superspace of whatever dimension using an extension of the Seitz notation as $\hat{g}_S = \{g_S, \delta|\mathbf{t}_S\}$, in which δ is -1 if the operator is primed, g_S is a $(3+d)\times(3+d)$ matrix and $\mathbf{t}_S$ is a translation vector referred to the direct superspace lattice. The invariance symmetry in $(3+d)$D of a crystal or magnetic structure means the verification of the two density invariance equations:

$$\rho_S(\{g_S, \delta|\mathbf{t}_S\}\mathbf{r}_S) = \rho_S(\mathbf{r}_S) \tag{54}$$

$$\mathbf{m}_S(\{g_S, \delta|\mathbf{t}_S\}\mathbf{r}_S) = \mathbf{m}_S(\mathbf{r}_S) \tag{55}$$

The δ part of the operator plays no role in the nuclear scattering density equation, but it is important in the magnetisation density to take into account the spin inversion when the symmetry operator is *primed*: $\delta = -1$.

The construction of the $\hat{g}_S = \{g_S, \delta|\mathbf{t}_S\}$ operators from the extended operators for the $(3+1)D$ case is given by the transformation:

$$\{g, \delta|\mathbf{t}, \tau\} \;\rightarrow\; \{g_S, \delta|\mathbf{t}_S\} \quad \mathbf{t} = (t_1, t_2, t_3) \quad t_4 = \tau + \mathbf{kt} \tag{56}$$

This allows naturally the use of the rules of crystallography for the action of these operators in direct and reciprocal spaces. For the case of a $(3+1)$D space, the $(3+d)\times(3+d)$, $d = 1$, matrix and translation parts have the following form:

$$g_S = \begin{pmatrix} g_{11} & g_{12} & g_{13} & 0 \\ g_{21} & g_{22} & g_{23} & 0 \\ g_{31} & g_{32} & g_{33} & 0 \\ h_{g1} & h_{g2} & h_{g3} & \epsilon_g \end{pmatrix} \qquad \mathbf{t}_S = (t_1, t_2, t_3, t_4) = (\mathbf{t}, \mathbf{t}_I) \tag{57}$$

Suppose two atoms (j) and (k) that are symmetry related through the operator $\hat{g}$ of the basic structure, such as $\hat{g}\bar{\mathbf{r}}_{jl} = g\bar{\mathbf{r}}_j + g\mathbf{R}_l + \mathbf{t} = \bar{\mathbf{r}}_k + \mathbf{R}_n$. In superspace, where points are described by coordinates $(x_{S1}, x_{S2}, x_{S3}, x_{S4})$, the action of the corresponding operator $\hat{g}_S$ on atom (j) is similar to that of $\hat{g}$ for the first three coordinates, but the last component is given by:

$$x_{S4}(k) = \mathbf{h}_g\bar{\mathbf{r}}(j) + \epsilon_g x_{S4}(j) + t_4 = \mathbf{h}_g\bar{\mathbf{r}}(j) + \epsilon_g x_{S4}(j) + \tau + \mathbf{kt} \tag{58}$$

We can see that this fourth coordinate depends on the three first coordinates of the atom (j) in the basic structure through $\bar{\mathbf{r}}(j)$.

In the general case, we have to consider that the physical space part of the operators $\hat{g}_S = \{g_S, \delta|\mathbf{t}_S\}$ when acting on modulation vectors like in (41) (for a single modulation vector the action is: $\hat{g}\mathbf{q} = \mathbf{q}g = \epsilon_g\mathbf{q} + \mathbf{h}_g$) the following matrix condition should be satisfied:

$$\begin{pmatrix} \sigma_{11} & \sigma_{12} & \sigma_{13} \\ \sigma_{21} & \sigma_{22} & \sigma_{23} \\ . & . & . \\ \sigma_{d1} & \sigma_{d2} & \sigma_{d3} \end{pmatrix} \begin{pmatrix} g_{11} & g_{12} & g_{13} \\ g_{21} & g_{22} & g_{23} \\ g_{31} & g_{32} & g_{33} \end{pmatrix} = \begin{pmatrix} \epsilon_{11} & \epsilon_{12} & \ldots & \epsilon_{1d} \\ \epsilon_{21} & \epsilon_{22} & \ldots & \epsilon_{2d} \\ . & . & \ldots & . \\ \epsilon_{d1} & \epsilon_{d2} & \ldots & \epsilon_{dd} \end{pmatrix} \begin{pmatrix} \sigma_{11} & \sigma_{12} & \sigma_{13} \\ \sigma_{21} & \sigma_{22} & \sigma_{23} \\ . & . & . \\ \sigma_{d1} & \sigma_{d2} & \sigma_{d3} \end{pmatrix} + \begin{pmatrix} h_{11} & h_{12} & h_{13} \\ h_{21} & h_{22} & h_{23} \\ . & . & . \\ h_{d1} & h_{d2} & h_{d3} \end{pmatrix} \tag{59}$$

or, in compact form,

$$\boldsymbol{\sigma}\mathbf{g} = \mathbf{E}_g\boldsymbol{\sigma} + \mathbf{H}_g \tag{60}$$

Where $\mathbf{g}$ is the conventional 3×3 rotational matrix of the physical space, the matrix $\boldsymbol{\sigma}$ of dimension $d \times 3$ is formed with the components of the modulation vectors referred to the reciprocal lattice of the physical space. The matrix $\mathbf{H}_g$ is formed by d reciprocal lattice vectors and the $d \times d$ matrix $\mathbf{E}_g$ contains only zeros and ± 1 describing how the modulation vectors are transformed by the operator $\hat{g}$. For modulations vectors pairs $(\mathbf{q}, -\mathbf{q})_p$ (with $p = 1, 2, \ldots, d$) not belonging to the same star, the matrix $\mathbf{E}_g$ is diagonal, with $E_g(i, i) = \pm 1$. We can extend the operators of $(3+1)D$ given in Eq. (57) for the general $(3+d)$D operator $\hat{g}_S = \{g_S, \delta|\mathbf{t}_S\}$, and write:

$$\hat{g}_S = \{g_S, \delta|\mathbf{t}_S\} \;\Rightarrow\; g_S = \begin{pmatrix} \mathbf{g} & \mathbf{0} \\ \mathbf{H}_g & \mathbf{E}_g \end{pmatrix} \quad \mathbf{t}_S = (t_1, t_2, \ldots t_{3+d}) = (\mathbf{t}, t_4, \ldots, t_{3+d}) = (\mathbf{t}, \mathbf{t}_I) \tag{61}$$

where $\mathbf{0}$ is a $3 \times d$ null matrix. Notice that δ must be taken into account for the action on magnetic moments that are inverted if the operator is primed ($\delta = -1$). In order to study the action of operators in superspace, it is convenient to introduce *augmented* matrices by adding a column with components of the associated translation vector as:

$$\hat{g}_S = \begin{pmatrix} \mathbf{g} & \mathbf{0} & \mathbf{t} \\ \mathbf{H}_g & \mathbf{E}_g & \mathbf{t}_I \\ 0 & 0 & 1 \end{pmatrix} \tag{62}$$

Notice that when we know the 3D operator matrix $\mathbf{g}$ and the modulation vectors, the matrices $\mathbf{H}_g$ and $\mathbf{E}_g$ can be easily calculated applying the relations (60). Using usual matrix operations, the action of the operator on a general vector position of superspace $\mathbf{r}_S = (\mathbf{r}_E, \mathbf{r}_I)$ is given by

$$\hat{g}_S\mathbf{r}_S = \begin{pmatrix} \mathbf{g} & \mathbf{0} & \mathbf{t} \\ \mathbf{H}_g & \mathbf{E}_g & \mathbf{t}_I \\ 0 & 0 & 1 \end{pmatrix} \begin{pmatrix} \mathbf{r}_E \\ \mathbf{r}_I \\ 1 \end{pmatrix} = \begin{pmatrix} \mathbf{g}\mathbf{r}_E + \mathbf{t} \\ \mathbf{H}_g\mathbf{r}_E + \mathbf{E}_g\mathbf{r}_I + \mathbf{t}_I \\ 1 \end{pmatrix} \tag{63}$$

For the action of operators in the modulation functions, we need the inverse of those operators. In Seitz notation, $\hat{g}_S^{-1} = \{g_S^{-1}, \delta| - g_S^{-1}\mathbf{t}_S\}$ ($\delta^{-1} = \delta$ always). The general expression of the inverse superspace symmetry operator is given by:

$$\hat{g}_S^{-1} = \begin{pmatrix} \mathbf{g}^{-1} & \mathbf{0} & -\mathbf{g}^{-1}\mathbf{t} \\ -\mathbf{E}_g^{-1}\mathbf{H}_g\mathbf{g}^{-1} & \mathbf{E}_g^{-1} & \mathbf{E}_g^{-1}\mathbf{H}_g\mathbf{g}^{-1}\mathbf{t} - \mathbf{E}_g^{-1}\mathbf{t}_I \\ 0 & 0 & 1 \end{pmatrix} = \begin{pmatrix} \mathbf{g}^{-1} & \mathbf{0} & -\mathbf{g}^{-1}\mathbf{t} \\ \mathbf{N}_g & \mathbf{E}_g^{-1} & -\mathbf{N}_g\mathbf{t} - \mathbf{E}_g^{-1}\mathbf{t}_I \\ 0 & 0 & 1 \end{pmatrix} \tag{64}$$

In general, a modulation vector can be decomposed as $\mathbf{q} = \mathbf{q}_r + \mathbf{q}_i$, where the subscripts 'r' and 'i' stand for *rational* and *irrational*, respectively. With an appropriate selection of the unit cell in the physical space, one can redefine the modulation

vectors so as to contain only zeroes and *irrational* components. In such cases, the matrix $\mathbf{H}_g$ is a null matrix and the calculations with operators simplify considerably. Selecting the appropriate centred cell for eliminating the rational components of the modulation vector, the symmetry operators in superspace simplify to:

$$\hat{g}_S = \begin{pmatrix} \mathbf{g} & \mathbf{0} & \mathbf{t} \\ \mathbf{0} & \mathbf{E}_g & \mathbf{t}_I \\ 0 & 0 & 1 \end{pmatrix} \qquad \hat{g}_S^{-1} = \begin{pmatrix} \mathbf{g}^{-1} & \mathbf{0} & -\mathbf{g}^{-1}\mathbf{t} \\ \mathbf{0} & \mathbf{E}_g^{-1} & -\mathbf{E}_g^{-1}\mathbf{t}_I \\ 0 & 0 & 1 \end{pmatrix} \tag{65}$$

The action of the inverse operator in $(3+d)$D superspace on a point corresponding to coordinates of the atom (k) in the basic structure gives another point corresponding to the atom (j), and we have:

$$\hat{g}_S^{-1}(\bar{\mathbf{r}}_k, \mathbf{r}_{Ik}) = (\bar{\mathbf{r}}_j, \mathbf{r}_{Ij}) = \big(\, \mathbf{g}^{-1}(\bar{\mathbf{r}}_k - \mathbf{t}), \quad \mathbf{N}_g(\bar{\mathbf{r}}_k - \mathbf{t}) + \mathbf{E}_g^{-1}(\mathbf{r}_{Ik} - \mathbf{t}_I) \,\big) \tag{66}$$

In practical applications, we need to know how these operators act on the modulation (structural displacement or magnetic moment) functions in order to allow the calculation of structure factors for structural analysis. The modulation functions of two symmetry-related atoms in the basic structure verifying $\hat{g}\bar{\mathbf{r}}_j = \bar{\mathbf{r}}_k + \bar{\mathbf{R}}_n$ are not independent if the corresponding superspace operator belongs to the symmetry of the modulated structure. Taking into account Eq. (66), the displacement modulation functions are transformed as:

$$\mathbf{u}_k[\mathbf{r}_I(k)] = \hat{g}\mathbf{u}_j[\mathbf{r}_I(j)] = g\mathbf{u}_j[\hat{g}^{-1}\mathbf{r}_I(j)] = g\mathbf{u}_j[\mathbf{N}_g(\bar{\mathbf{r}}(j) - \mathbf{t}) + \mathbf{E}_g^{-1}(\mathbf{r}_I(j) - \mathbf{t}_I)] \tag{67}$$

For the case of magnetic moments, the action is as:

$$\mathbf{m}_k[\mathbf{r}_I(k)] = \hat{g}\mathbf{m}_j[\mathbf{r}_I(j)] = \delta\det(g)g\mathbf{m}_j[\hat{g}^{-1}\mathbf{r}_I(j)] = \delta\det(g)g\mathbf{m}_j[\mathbf{N}_g(\bar{\mathbf{r}}(j) - \mathbf{t}) + \mathbf{E}_g^{-1}(\mathbf{r}_I(j) - \mathbf{t}_I)] \tag{68}$$

or, in a more simple form, putting the argument of $\mathbf{m}_k$ in terms of that of $\mathbf{m}_j$, as:

$$\mathbf{m}_k[(\mathbf{H}_g\bar{\mathbf{r}}_j + \mathbf{E}_g\mathbf{r}_I(j) + \mathbf{t}_I)] = \delta\det(g)g\mathbf{m}_j(\mathbf{r}_I(j)) \tag{69}$$

These equations are the basis for calculating the constraints on modulation functions imposed by symmetry in special positions of the basic structure.

8.4. Structure factors in superspace

The crystallographic $(3+d)$D superspace groups, for dimensions $d = 1$, 2, and 3, have been tabulated recently [90] in form of a database, the number of superspace groups being 775, 3338, and 12 584 respectively. The magnetic superspace groups have not yet been tabulated and their number is still unknown.[9] The symbols used for designing a superspace group is based on the Hermann–Mauguin notation of the parent crystallographic group followed by the modulation vector and a set of letters indicating the translation in the internal space. In principle, one can use the same kind of notation for magnetic superspace groups using primed symbols. For instance, the crystallographic space group noted $Pnma(00\gamma)0s0$ can be easily constructed by calculating the augmented matrices of the generators n, m, a using the rules (60) and putting the internal translation of the $\hat{g}_S(m)$ equal to $s = 1/2$, $t_{S4} = 1/2$ and zero for the other generators.

The detailed calculation of structure factors for modulated crystal and magnetic structures is out of the scope of this paper; the reader can find detailed discussions, references, and examples in the papers [81,89,91,92] for the case of crystal structures. There is no similar development for magnetic structure factors; however, their inclusion in the appropriate formula is straightforward. The most general expression for calculating structure factors of modulated crystal structures has been provided for the first time by Akiji Yamamoto [89]. It is formulated directly in superspace, so that the application of symmetry is straightforward: formula (15) in [89]. The treatment in superspace implies that the summations for the whole crystal are transformed in integrations over the internal space of modulation functions, taking into account that they are periodic of period 1. Here we provide a simplified formula (considering only displacive modulations and neglecting the temperature factor) for the case of the nuclear structure factor and an equivalent expression for the magnetic structure factor:

$$F(\mathbf{H}_S) = \sum_{j=1}^{n_a} O_j b_j \sum_{s=1}^{|\mathcal{G}_S|} \int_0^1 \mathrm{d}\bar{x}_4^j \ldots \int_0^1 \mathrm{d}\bar{x}_{3+d}^j \exp[2\pi\mathrm{i}\mathbf{H}_S\hat{g}_S^s\mathbf{r}_S^j(\bar{x}_4^j, \ldots \bar{x}_{3+d}^j)] \tag{70}$$

[9] Very recently H. Stokes and B. Campbell have made available a provisional list up to dimension $d = 3$ containing a total of 347 975 magnetic superspace groups. See https://stokes.byu.edu/iso/ssg.php.

The corresponding equation for the magnetic structure factor of a crystal having displacive and magnetic modulation is:

$$\mathbf{M}(\mathbf{H}_S) = p \sum_{j=1}^{m_a} O_j f_j(H_S) \sum_{s=1}^{|\mathcal{G}_S|} \int_0^1 d\bar{x}_4^j \ldots \int_0^1 d\bar{x}_{3+d}^j \quad \hat{g}_S^s \mathbf{m}_S^j(\bar{x}_4^j, \ldots \bar{x}_{3+d}^j) \exp[2\pi i \mathbf{H}_S \hat{g}_S^s \mathbf{r}_S^j(\bar{x}_4^j, \ldots \bar{x}_{3+d}^j)] \tag{71}$$

where $|\mathcal{G}_S|$ is the order of the point group of the superspace group $\mathcal{G}_S$ and the superscript s numbers the different symmetry operators of $\mathcal{G}_S$. The first sum for $F(\mathbf{H}_S)$ is extended to all atoms in the asymmetric unit, whereas the corresponding sum for $\mathbf{M}(\mathbf{H}_S)$ is extended only to magnetic atoms. The scattering length of atom j is b_j and the magnetic form factor is $f_j(H_S)$. We have made explicit only the dependence on the internal space of the modulation functions, of course the vectors in superspace contain also the external components. For practical applications, the modulation functions should be written in terms of their development in Fourier series like (47). The structural parameters become then the cosine and sine amplitudes, which are constant vectors with components to be adjusted against experimental data. A recent example of magnetic structure determination using the superspace approach is the case of the multiferroic compound α-$NaFeO_2$ [93].

9. Computing tools for determination and analysis of magnetic structures

9.1. The pioneering times

During many years, the people needing determining magnetic structures were working using *ad hoc* computing programs or making calculations by hand for relatively simple crystal structures. For neutron powder diffraction, the first general computing program able to work with commensurable magnetic structures was that provided by H.M. Rietveld [94]. Hewat's Fortran version [95] of this program was available at the ILL from 1980 onwards. The user had to construct him(her)self the magnetic model, using physical intuition or the knowledge on magnetic symmetry (representation analysis or Shubnikov groups) and translate this model into the input file of the program. No control of the model correctness was performed by the program.

For single crystals, the system *The Cambridge Crystallography Subroutine Library* [96] was, and still is, one of the most complete set of procedures for handling magnetic single crystal diffraction. Its scope is very well summarised by the following words of the authors:

The Cambridge Crystallography Subroutine Library (CCSL) is a set of subroutines which are used in the construction of Fortran crystallographic programs. CCSL has been written with the needs of the nonstandard crystallographer in mind. [...] the aim of CCSL is to allow each user to do something a little different, and to experiment with his own ideas using the subroutines in the library for the routine parts of the calculations.

Together with many programs and utilities for crystallographic applications, the magnetic programs based on CCSL are able to treat single crystal diffraction data (polarised and unpolarised neutrons) and, to a limited extent, powder diffraction. For instance, the program MAGLSQ allows the refinement of magnetic structures (commensurable and incommensurable) as well as the treatment of flipping ratios for spin densities. The program CHILSQ has been designed for the refinement of local susceptibility tensors using polarised neutrons and flipping ratios measurements. The programs PALSQ and PAXLSQ are able to treat polarimetry data under zero field for determining fine details of magnetic structures. Presently, the full set of programs can be freely downloaded from the website given in reference [96].

9.2. The last thirty years

The original Rietveld [94] program was limited to commensurable magnetic structures, but his idea gave rise to a series of computing programs, using the Rietveld method, that extended the initial capabilities. At the end of the 1990s, there were several Rietveld programs and the way of using them, in the form of guidelines, was published in a paper of the Powder Diffraction Commission of the IUCr[10] [97]. Those able to handle magnetic structures were, from the beginning, the programs GSAS [98] and RIETAN [99,100]. The most recent versions of those programs are able to work with commensurable magnetic structures. In the case of RIETAN, there are strong limitations because magnetic groups are not implemented. In the latest versions of GSAS (GSAS-II) [98], the Shubnikov groups are fully implemented. More recently, the commercial program TOPAS [101] has included the possibility to work with commensurable magnetic structures.

For working with incommensurable magnetic structures, the program SIMREF [102], published in 1988, was developed later to include this option; however, its use has been only testimonial. The program *FullProf* was developed at ILL at the end of the 1980s by the first author of this paper. It was based on DBW [103], a popular application for working with X-ray powder diffraction distributed freely from 1981 onwards. The genesis of *FullProf* started in the middle of the 1980s with strong modifications of the DBW program and finally with the introduction of magnetic structures using the formalism of propagation vectors in 1990. The first published description of features available in *FullProf* for incommensurable magnetic

[10] IUCr: International Union of Crystallography.

structures was done in [66]. In that article, there was also the first description of the program *MagSan* for determining commensurable magnetic structures using Simulated Annealing, later included in the *FullProf Suite* for general crystal and magnetic structures. By the middle–end of the 1990s, three programs [104–106], MODY, SARAh, and *BasIreps* (this last included within the *FullProf Suite*) were released for helping to determine magnetic structures. These programs use the representation analysis popularised by Bertaut [40] and were distributed and used by the community. The *FullProf Suite* is being developed permanently and it is currently the most used set of program for handling magnetic structures using powder or single crystal neutron diffraction data.

A series of computing tools for crystallography, including magnetic structures, are available at the Bilbao Crystallographic Server (BCS) [107]. This is a web application that is very intuitive, and the user can consult everything related with space crystal and magnetic groups. Programs for making transformation between different settings, determination of subgroups and coset decompositions are made available to non-specialists. They can output Crystallographic Information Files (CIF) that serve as exchange of crystallographic data and structures. The most important programs for magnetic structure determination and analysis are MAGMAGN and *k*-SUBGROUPS [108]; they are able to output magnetic CIF that can be read immediately by other programs like *FullProf*, JANA or GSAS-II. Moreover, they provide for the first time a database of determined magnetic structures [109,110] that the user can inspect and download, which are accompanied by visualisation capabilities through the program JMol [111].

For incommensurable crystal structures, two programs for single crystals were developed from the middle of the 1980s: REMOS [112] and JANA [113]. JANA-2006 was the first program that incorporated the treatment of incommensurable magnetic structures using superspace groups. Whereas this formalism is not yet in the common culture of condensed matter physicists working on magnetism, a strong progress is being accomplished in the last years thanks to the contribution of web applications using data bases [90,114]. A huge amount of work on symmetry has been developed by H. Stokes, D. Hatch, and B. Campbell. Stokes developed the computing system ISOTROPY [115], in which many algorithms for working with space groups, representations and symmetry modes, are implemented. Together with the programs, they have made available databases to be used by external software. In particular some applications of the BCS and the *FullProf Suite* use the databases of Shubnikov groups [80] and *irreps* [116]. The program ISODISTORT is a web application interfacing ISOTROPY and works making an analysis of a paramagnetic group together with a series of propagation (modulation). The program calculates the *irreps* and isotropy subgroups, providing symmetry modes and the (super)space groups corresponding to different selections of the *irreps* and order parameter directions. For the case of commensurable structures, the program outputs directly a template file to be used by *FullProf* or by TOPAS. An account of the current state of methods and tools has been published recently by F. Damay of the LLB [117].

A very recent program for analysing polarimetry and integrated intensity data on single crystals has been developed at ILL by N. Qureshi using a modern graphic user interface that facilitates the precise determination of magnetic structures [118].

It is clear that the computing tools for helping determination of magnetic structures will increase in the forthcoming months and years. In particular, the full implementation within the *FullProf Suite* of superspace formalism is planed. Presently, this approach for incommensurable magnetic structures is already implemented, but only within a commensurable crystallographic structure. Using the same library recently developed [119] for working with general crystallographic groups, appropriate utilities for working with superspace will also be implemented at the BCS.

10. Conclusions

We have presented a general overview of the field of magnetic structures in crystals emphasising the microscopic origin of magnetic ordering, the expressions for calculating neutron scattering amplitudes (structure factors) and summarising the symmetry concepts necessary for analysing experimental data.

Finally, we want to stress that the impact of this field in solid-state physics and chemistry is increasing thanks to the need of understanding new materials showing interesting physical properties (giant magneto-resistance, frustrated magnetism, spin ices, multiferroics, etc.). The knowledge of the magnetic ground state of new materials provides new insights into the electronic properties of solids and helps to challenge *ab initio* codes of electronic structure for predicting magnetic ordering from first principles, which is still in its infancy.

With the objective of developing this field, the IUCr created, in the frame of the Twenty-Second Congress and General Assembly of the International Union of Crystallography (Madrid 2011), the Commission on Magnetic Structures [120], which is trying to unify the different descriptions of magnetic structures and has developed a format for a new CIF for both commensurable and incommensurable magnetic structures.

The authors are grateful to Isabelle Mirebeau and Frédéric Bourdarot for their critical reading of the manuscript.

Appendix A. The Rudermann–Kittel interaction

The main part of the Hamiltonian is the free electron Hamiltonian, assumed to form a single band for simplicity:

$$\mathcal{H}_0 = \sum_{k\sigma} \epsilon_k c^*_{k\sigma} c_{k\sigma} \tag{72}$$

where $c^*_{k\sigma}$ and $c_{k\sigma}$ respectively create and destroy a conduction electron of wave vector $\mathbf{k}$ and spin component $\sigma = +$ or $-$ along a particular direction z.

In addition, there is a perturbation, which is the interaction of conduction electrons with the localised electron spins $\mathbf{S}_i$. It is a good approximation to assume that the interaction is local, i.e. the spin $\mathbf{S}_i$ localised at site i interacts only with the spin $\mathbf{s}_i$ of the conduction electron at site i, if there is one. The perturbation may be assumed to have the form

$$\mathcal{H}_1 = \lambda \sum_i \mathbf{S}_i \cdot \mathbf{s}_i \tag{73}$$

The spin $\mathbf{s}_i$ will now be expressed in terms of the operators $c^*_{i\sigma}$ and $c_{i\sigma}$, Fourier transforms of $c^*_{k\sigma}$ and $c_{k\sigma}$ where $\sigma = +$ or $-$. According to the Pauli principle, the site i can accommodate either no conduction electron, or two conduction electrons of opposite spins, or one conduction electron of spin $+$, or one conduction electron of spin $-$. In all four cases, it is readily seen that $s^z_i = (c^*_{i+}c_{i+} - c^*_{i-}c_{i-})/2$, $s^+_i = c^*_{i+}c_{i-}$ and $s^-_i = c^*_{i-}c_{i+}$. It follows after a few lines' calculation that (73) reads

$$\mathcal{H}_1 = \frac{\lambda}{2} \sum_{i\sigma\sigma'} S^{\sigma\sigma'}_i c^*_{i\sigma} c_{i\sigma'} = \frac{\lambda}{2N} \sum_{ikk'\sigma\sigma'} S^{\sigma\sigma'}_i c^*_{k\sigma} c_{k'\sigma'} \exp[i(\mathbf{k}-\mathbf{k}')\cdot\mathbf{R}_i] \tag{74}$$

where

$$S^{\sigma\sigma}_i = S^z_i \sigma, \qquad S^{+-}_i = S^-_i, \qquad S^{-+}_i = S^+_i \tag{75}$$

For $\lambda = 0$, the conduction electrons are in their ground state $|\,0\rangle$ characterised by $c^+_{k\sigma}c_{k\sigma}\,|\,0\rangle = |\,0\rangle$ if $\epsilon_k < \epsilon_F$ and $c^+_{k\sigma}c_{k\sigma}\,|\,0\rangle = 0$ if $\epsilon_k > \epsilon_F$. If the N localised spins $\mathbf{S}_i$ of modulus s are taken into account, the $(2s+1)^N$ corresponding states have the same energy E_0, so that there is a ground space $\mathcal{E}_0$, which is $(2s+1)^N$ times degenerate. The case of interest is when λ is small but does not vanish. Then there are $(2s+1)^N$ low-energy eigenstates $|\,\psi\rangle$ of $\mathcal{H} = \mathcal{H}_0 + \mathcal{H}_1$, which are close to the space $\mathcal{E}_0$. Using second-order perturbation theory, it can be shown that their projection $\mathcal{P}_0\,|\,\psi\rangle$ onto $\mathcal{E}_0$ are the eigenstates of

$$\mathcal{H}_{eff} = \mathcal{P}_0 \mathcal{H}_1 (E_0 - \mathcal{H}_0 - i\eta)^{-1} \mathcal{H}_1 \mathcal{P}_0 \tag{76}$$

where the limit $\eta \to 0$ has to be taken. For $\eta = 0$ the inverse operator is not defined. Because of the projection operator $\mathcal{P}_0$, this Hamiltonian depends only on the localised spin operators $\mathbf{S}_i$, while conduction electrons are in their ground state $|\,0\rangle$. From now on, the projection operator will be omitted; we shall keep in mind that the conduction electrons are in their ground state, and $\mathcal{H}_{eff}$ will be considered a function of the localised spin operators. Using (76), (74) and (72), one obtains, assuming a single magnetic atom per unit cell

$$\mathcal{H}_{eff} = \frac{\lambda^2}{4} \sum_{ij\sigma\sigma' kk'} S^{\sigma\sigma'}_i S^{\sigma'\sigma}_j \sum_{kk'} \langle 0\,|\,c^*_{k\sigma}c_{k'\sigma'} \frac{1}{\epsilon_k - \epsilon_{k'}} c^*_{k'\sigma'}c_{k\sigma}\,|\,0\rangle \exp[i(\mathbf{k}-\mathbf{k}')\cdot\mathbf{R}_{ij}] \tag{77}$$

where $\mathbf{R}_{ij}$ is the vector connecting sites i and j. The matrix element is a function $K(\mathbf{k},\mathbf{k}')$ independent of σ and σ'. According to (75), relation (77) reads

$$\mathcal{H}_{eff} = -\sum_{ij} J_{ij} \mathbf{S}_i \cdot \mathbf{S}_i$$

where

$$J_{ij} = -\frac{\lambda^2}{2} \sum_k \sum_{k'} K(\mathbf{k},\mathbf{k}') \exp[i(\mathbf{k}-\mathbf{k}')\cdot\mathbf{R}_{ij}] \tag{78}$$

The exploitation of this formula is a mathematical exercise that will be performed in some detail assuming that ϵ_k depends only on $k = |\mathbf{k}|$ (an assumption that is not realistic at all, but simplifies the calculation, which can be extended to the realistic case). Formula (78) reads

$$J_{ij} = J(R_{ij}) = -\frac{\lambda^2}{2} \sum_{k<k_F} \sum_{k'>k_F} \frac{1}{\epsilon_k - \epsilon_{k'}} \exp[i(\mathbf{k}-\mathbf{k}')\cdot\mathbf{R}_{ij}]$$

Introducing the polar coordinates k, θ, φ and k', θ', φ' of $\mathbf{k}$ and $\mathbf{k}$', and integrating on φ and φ', one obtains

$$J(R) = -2\pi^2\lambda^2 \int_{k<k_F} \int_{k'>k_F} \mathrm{d}k\,\mathrm{d}k' \frac{k^2 k'^2}{\epsilon_k - \epsilon_{k'}} \int_{-\pi}^{\pi} \mathrm{d}\theta \int_{-\pi}^{\pi} \mathrm{d}\theta' \sin\theta \sin\theta' \exp[\mathrm{i}kR\cos\theta - \mathrm{i}k'R\cos\theta']$$

or, after integration over θ and θ':

$$J(R) = \frac{8\pi^2\lambda^2}{R^2} \int_{k<k_F} \int_{k'>k_F} \mathrm{d}k\,\mathrm{d}k' \frac{kk'}{\epsilon_k - \epsilon_{k'}} \sin kR \sin k'R = J_1(R) + J_2(R) \tag{79}$$

where

$$J_1(R) = -\frac{4\pi^2\lambda^2}{R^2} \int_{k<k_F} \int_{k'>k_F} kk'\mathrm{d}k\,\mathrm{d}k' \frac{\cos(k+k')R}{\epsilon_k - \epsilon_{k'}} \tag{80}$$

and

$$J_2(R) = \frac{4\pi^2\lambda^2}{R^2} \int_{k<k_F} \int_{k'>k_F} kk'\mathrm{d}k\,\mathrm{d}k' \frac{\cos(k-k')R}{\epsilon_k - \epsilon_{k'}} \tag{81}$$

It will be appropriate to introduce the variables $u = k' - k$ and $v = k' + k - 2k_F$, which satisfy the relations $u \geq 0$ and $-u \leq v \leq u$. After integration over v, $J_1(R)$ turns out to be the Fourier transform of a function of u that has a singularity at $u = 0$ but is analytic everywhere else. After integration over u, $J_2(R)$ turns out to be the Fourier transform of an analytic function of v.

At this point, it is appropriate to recall some general properties of the Fourier transformation. The Fourier transform $\mathcal{J}(\mathbf{k})$ of a short-ranged $J(R)$ is an analytic function of $\mathbf{k}$, since it is a finite sum of analytic functions. Conversely, the inverse Fourier transform of an analytic function $\mathcal{J}(\mathbf{k})$ is short ranged (or decays rapidly, e.g., exponentially). Therefore, if we are interested in the long-distance behaviour of $J(R)$ given by (79), we can ignore the component $J_2(R)$, which is the Fourier transform of an analytic function. Moreover, in the expression (80) of $J_1(R)$, all quantities can be replaced by their expression in the neighbourhood of $u = v = 0$, except for the rapidly fluctuating factor $\cos(k + k')R = \cos(2k_F + v)R$. Thus, at long distance,

$$J(R) \simeq J_1(R) = \frac{4\pi^2\lambda^2}{R^2} \int_{u>0} \mathrm{d}u \int_{-u}^{u} k_F^2 \frac{\cos(2k_F + v)R}{Bu}\,\mathrm{d}v \tag{82}$$

where $B = \mathrm{d}\epsilon_k/\mathrm{d}k$ at k_F. Integration yields

$$J(R) = \frac{4\pi^2\lambda^2}{BR^2} k_F^2 \cos 2k_F R \int_{u>0} \frac{\mathrm{d}u}{u} \int_{-u}^{u} \cos vR\,\mathrm{d}v$$

or

$$J(R) = \frac{8\pi^2\lambda^2}{BR^3} k_F^2 \cos(2k_F R) \int_0^\infty \frac{\sin(uR)}{u}\,\mathrm{d}u = \frac{8\pi^3\lambda^2}{BR^3} k_F^2 \cos(2k_F R) \tag{83}$$

which is formula (9).

Appendix B. The Devil's staircase

The minimum of expression (11) must satisfy the equations

$$\frac{\partial}{\partial\varphi_n}\mathcal{H} = 2\varphi_n - \varphi_{n+1} - \varphi_{n-1} + \lambda \sin\varphi_n = 0 \quad (n \neq 1, N) \tag{84}$$

These equations are independent of μ. The equations for $n = 1$ and N, which depend on μ, will be provisionally ignored.

If $\lambda = 0$, the solutions to (84) are $\varphi_n = n\alpha + \theta$, depending on the two parameters α and θ. When λ does not vanish, yet small, it is convenient to write $\varphi_n = n\alpha + u_n + \theta$, where α and θ are arbitrary and u_n is small.

Equations (84) read

$$u_{n+1} + u_{n-1} - 2u_n = \lambda \sin(n\alpha + u_n + \theta) \tag{85}$$

The left-hand side has the form $G\,|\,u\rangle$, where G is a $N \times N$ matrix and $|\,u\rangle$ is a column matrix with N elements. Introducing the inverse matrix Γ of G, (85) reads

$$u_n = \lambda \sum_{n'} \Gamma(n - n') \sin(n'\alpha + u_{n'} + \theta) \tag{86}$$

For any given value of α, the solution is obviously a periodic function of θ with period 2π. Equations (86) can be solved by iteration, assuming the initial value $u_n^{(0)} = 0$. After p iteration steps, the obtained solution $u_n^{(p)}$ is correct to order μ^p. It depends on α and θ, and the energy should be minimised with respect to α and θ. For a given value of α, the energy is a continuous function of θ at all iteration steps and, if the iteration converges, the final result should be a continuous function of θ.

If a solution to (86) is known for given values α and θ, another solution for the same α is obtained if u_n is substituted by u_{n+m}, where m is any integer: $u_{n+m} = \lambda \sum_{n'} \Gamma(n+m-n') \sin(n'\alpha + u_{n'+p} + \theta)$ or $u_n = \lambda \sum_{n'} \Gamma(n+p-n') \sin(n'\alpha + u_{n'} - m\alpha + \theta)$. This solution has the same energy as the initial one, $E(\alpha,\theta) = E(\alpha, \theta - m\alpha)$. If α/π is not a rational number, the values $\theta - m\alpha$ generate an infinite number of values, which correspond to the same energy $E(\alpha, \theta - m\alpha) = E(\alpha,\theta)$. For any value θ', one can find integers p and k such that $|\theta - m\alpha - \theta' - 2\pi k|$ is smaller than any small positive number ϵ. Since $E(\alpha,\theta)$ is assumed to be a continuous function of θ, $E(\alpha,\theta')$ should be equal to $E(\alpha,\theta)$. We conclude that $E(\alpha,\theta)$ is independent of θ if α/π is irrational.

If $\alpha/2\pi$ is a rational number p/q (where p and q are integers without common factor) $E(\alpha,\theta)$ is still equal to $E(\alpha, \theta - m\alpha)$ and also to $E(\alpha, \theta + 2k\pi)$, i.e. $E(\alpha,\theta) = E(\alpha, \theta - \alpha + 2k\pi) = E(\alpha, \theta - 2\alpha + 2k\pi) = E(\alpha, \theta - 3\alpha) = \ldots = E(\alpha, \theta - (q-1)\alpha + 2k\pi)$, but the sequence stops there since $q\alpha = 2p\pi$. The energy $E(\alpha,\theta)$ is now a periodic function of θ with period $2\pi/q$. It has a minimum E_m for some value θ_0 of θ and a maximum E_M for another value. When α is infinitely close to $p\pi/q$, the structure is locally similar to the 'rational' structure corresponding to a value of θ that changes with n, so that the energy density fluctuates in space between E_m and E_M, and the average energy density E satisfies $E_\mathrm{m} < E < E_\mathrm{M}$. For that reason, even if μ is slightly different from the value at which the rational value $\alpha = p\pi/q$ would minimise the energy for $\lambda = 0$, it still minimises the energy for $\lambda \neq 0$. Commensurate structures have a non-vanishing domain of stability!

It will now be explained why the transition from a commensurable structure $\alpha = p\pi/q$ to something else is continuous. Let $\varphi_n^{(0)} = n\alpha + u_n^{(0)} + \theta_0$ be the commensurable structure that minimises the energy when μ is close to a certain value μ_0. We wish to know the energy when φ_n is slightly different from $\varphi_n^{(0)}$. However, it is convenient to select the sites $n = q\nu$, which are equivalent in the commensurable structure. The integer ν takes the values $1, 2, 3, \ldots N/q$. We therefore introduce the variables $v_\nu = \varphi_{q\nu} - \varphi_{q\nu}^{(0)}$ and we define the minimum $W(v_1, v_2, v_3, \ldots)$ for given values of $v_1, v_2, v_3, \ldots$. Even though we are not able to calculate it, we may guess how it looks like for small deviations $v_\nu - v_{\nu-1}$. The sum of the first two terms of expression (11) can be written as an algebraic expression $A\sum(v_\nu - v_{\nu-1})^2$, where linear terms are absent for a suitable choice μ_0 of μ, higher-order terms are negligible for small deviations, and interactions for $|\nu - \nu'| < 1$ are ignored for the sake of simplicity. The last term of expression (11) is a periodic function of period $2\pi/q$. It will be written as the first term of a Fourier series, $-B\sum\cos(qv_\nu - \delta)$, where the constant δ is zero because the energy minimum corresponds to $v_\nu = 0$. Thus the energy is phenomenologically written as

$$W = \frac{A}{2}\sum_\nu (v_\nu - v_{\nu-1})^2 - B\sum_\nu \cos qv_\nu - \delta\mu \sum_\nu (v_\nu - v_{\nu-1}) \tag{87}$$

where $\delta\mu = \mu - \mu_0$.

The minimum of (87) satisfies

$$A(v_{\nu+1} + v_{\nu-1} - 2v_\nu) = B\sin qv_\nu \quad (\nu \neq 1, N/q) \tag{88}$$

This is a discrete, time-independent form of the sine Gordon equation. It has the solution v_ν, which minimises (87) when $\delta\mu = 0$. When $\delta\mu$ increases and reaches a critical value $\delta\mu_c^+$, the first non-uniform solution that appears corresponds to a domain wall (called discommensuration in this case, or sometimes soliton). A discommensuration centred at ν_0 has the following properties:

$$v_\nu = 0 \quad (\nu << \nu_0), \qquad v_\nu = 2\pi \quad (\nu >> \nu_0) \tag{89}$$

For $\delta\mu = 0$, the discommensuration has an energy w_0 proportional to $\sqrt{AB}$. When $\delta\mu$ becomes equal to $\delta\mu_c^+ = w_0$, the structure with one discommensuration has the same energy as the commensurable structure. When $\delta\mu$ is slightly larger than $\delta\mu_c^+$, several discommensurations form. Let $\Delta\nu$ be their distance. Within this distance, the increment v must go from the value $2P\pi$ (where P is an integer) to the value $2(P+1)\pi$. In the case of a single discommensuration, v goes from $2P\pi$ to $2(P+1)\pi$ on an infinite distance. In other words, the minimum energy of a discommensuration corresponds to $\Delta\nu = \infty$. If there are several discommensurations, $\Delta\nu$ must be finite and this costs energy: the energy increases faster than the number of discommensurations. For that reason, the number of discommensurations increases continuously with $\delta\mu$: the transition at $\delta\mu_c^+$ is continuous. Of course, when $\delta\mu$ is negative and decreases, there is also a continuous transition at some value $\delta\mu_c^-$.

Let the repulsive interaction between discommensurations be more precisely described. Far from ν_0, Eq. (87) takes the linear form $A(v_{\nu+1} + v_{\nu-1} - 2v_\nu) = Bqv_\nu$, the solution to which is

$$v_\nu = Const \times \exp(-\kappa|\nu - \nu_0|) \tag{90}$$

with $\kappa = \sqrt{Bq/A}$. This exponential decay implies an exponential decay of the interaction between discommensurations. The energy of a system of discommensurations at distance $\Delta\nu$ is

$$W = \frac{N}{q\Delta\nu}[w_0 + w_1 \exp(-\kappa\Delta\nu) - 2\pi\delta\mu] \tag{91}$$

Its minimum is given by $\mathrm{d}W/\mathrm{d}\Delta\nu = 0$, i.e.

$$\Delta\nu = \frac{2\pi\delta\mu - w_0}{w_1}\exp(\kappa\Delta\nu)$$

or

$$\kappa\Delta\nu \approx \ln\frac{w_1}{2\pi\delta\mu - w_0} \tag{92}$$

Appendix C. Classical mean-field approximation to the first ordered state

The interaction energy between the spins i and j located respectively in the unit cells n and m, is supposed to be of the form:

$$E_{ij}(\mathbf{R}_n, \mathbf{R}_m) = -\mathbf{S}_i(\mathbf{R}_n)\mathbf{J}_{ij}(\mathbf{R}_n, \mathbf{R}_m)\mathbf{S}_j(\mathbf{R}_m) \tag{93}$$

$$E_{ij}(\mathbf{R}_n, \mathbf{R}_m) = -\sum_{\alpha\beta} S_i^{\alpha}(\mathbf{R}_n)\, J_{ij}^{\alpha\beta}(\mathbf{R}_n, \mathbf{R}_m) S_j^{\beta}(\mathbf{R}_m) \tag{94}$$

The translation symmetry of the crystal implies that

$$\mathbf{J}_{ij}(\mathbf{R}_n, \mathbf{R}_m) = \mathbf{J}_{ij}(\mathbf{R}_n - \mathbf{R}_p, \mathbf{R}_m - \mathbf{R}_p) \;\Rightarrow\; \mathbf{J}_{ij}(\mathbf{R}_n, \mathbf{R}_m) = \mathbf{J}_{ij}(\mathbf{R}_n - \mathbf{R}_m, 0) \tag{95}$$

Let us assume that the orientation distribution function of the spin i is normalised to 1 over all solid angles, so that average values of any quantity can be directly obtained by multiplying by the distribution function and integrating over all orientations:

$$\int p_i(\boldsymbol{\omega}_i)\,\mathrm{d}\boldsymbol{\omega}_i = 1 \quad \boldsymbol{\omega}_i = (\theta_i, \phi_i) \tag{96}$$

The internal energy and the entropy of the spin system are given by the equations:

$$U = \frac{1}{2}\sum_{ij}\int \mathrm{d}\boldsymbol{\omega}_i \int \mathrm{d}\boldsymbol{\omega}_j\, p_i(\boldsymbol{\omega}_i) p_j(\boldsymbol{\omega}_j) E_{ij}(\boldsymbol{\omega}_i, \boldsymbol{\omega}_j) \tag{97}$$

$$S = -k_B \sum_i \int \mathrm{d}\boldsymbol{\omega}_i\, p_i(\boldsymbol{\omega}_i) \ln p_i(\boldsymbol{\omega}_i) \tag{98}$$

The minimisation of the free energy with respect to all p_i at temperature T (defining $\beta_{\mathrm{B}} = \frac{1}{k_{\mathrm{B}}T}$) gives the set of coupled equations:

$$p(\boldsymbol{\omega}_i) = \frac{\mathrm{e}^{-\beta_{\mathrm{B}}\sum_j \int \mathrm{d}\boldsymbol{\omega}_j p_j(\boldsymbol{\omega}_j) E_{ij}(\boldsymbol{\omega}_i, \boldsymbol{\omega}_j)}}{\int \mathrm{d}\boldsymbol{\omega}_i\, \mathrm{e}^{-\beta_{\mathrm{B}}\sum_j \int \mathrm{d}\boldsymbol{\omega}_j p_j(\boldsymbol{\omega}_j) E_{ij}(\boldsymbol{\omega}_i, \boldsymbol{\omega}_j)}} \tag{99}$$

We can put the above equation in terms of the average spins (magnetic moment) by integrating for all solid angles and defining:

$$\mathbf{m}_i(\mathbf{R}_n) = \int \mathrm{d}\boldsymbol{\omega}_i^{\mathbf{R}_n}\, p_i(\boldsymbol{\omega}_i^{\mathbf{R}_n}) \mathbf{S}_i(\mathbf{R}_n) \tag{100}$$

For a uniform distribution $p_i(\boldsymbol{\omega}_i) = \frac{1}{4\pi}$, the value of the average moment corresponds to the paramagnetic state and $\mathbf{m}_i(\mathbf{R}_n) = \mathbf{0}$ for all sites in the crystal. Replacing the energy terms in the above equations by its expression for the general case:

$$E_{ij}(\boldsymbol{\omega}_i^{\mathbf{R}_n}, \boldsymbol{\omega}_j^{\mathbf{R}_m}) = -\sum_{\alpha\beta} S_i^{\alpha}(\mathbf{R}_n)\; J_{ij}^{\alpha\beta}(\mathbf{R}_n, \mathbf{R}_m)\; S_j^{\beta}(\mathbf{R}_m) \tag{101}$$

we obtain the following expression for the average spin of atom i at the unit cell n:

$$\mathbf{m}_i(\mathbf{R}_n) = \int \mathrm{d}\boldsymbol{\omega}_i^{\mathbf{R}_n} p_i(\boldsymbol{\omega}_i^{\mathbf{R}_n}) \mathbf{S}_i(\mathbf{R}_n) = \frac{\int \mathrm{d}\boldsymbol{\omega}_i^{\mathbf{R}_n} \mathbf{S}_i(\mathbf{R}_n)\, \mathrm{e}^{\beta_\mathrm{B} \mathbf{S}_i(\mathbf{R}_n)\mathbf{H}_{in}}}{\int \mathrm{d}\boldsymbol{\omega}_i^{\mathbf{R}_n}\, \mathrm{e}^{\beta_\mathrm{B} \mathbf{S}_i(\mathbf{R}_n)\mathbf{H}_{in}}} \tag{102}$$

where we have defined the molecular field at the site i, n by the vectorial equation:

$$\mathbf{H}_{in} = \sum_{jm} \mathbf{J}_{ij}(\mathbf{R}_n - \mathbf{R}_m)\mathbf{m}_j(\mathbf{R}_m) \tag{103}$$

or in components:

$$H_{in}^{\alpha} = \sum_{jm\beta} J_{ij}^{\alpha\beta}(\mathbf{R}_n - \mathbf{R}_m) m_j^{\beta}(\mathbf{R}_m) \tag{104}$$

The non-linear mean-field coupled equations in $\mathbf{m}_i(\mathbf{R}_n)$ cannot be solved easily. It is clear by looking at the explicit expression

$$\mathbf{m}_i(\mathbf{R}_n) = \frac{\int \mathrm{d}\boldsymbol{\omega}_i^{\mathbf{R}_n} \mathbf{S}_i(\mathbf{R}_n)\, \mathrm{e}^{\beta_\mathrm{B} \mathbf{S}_i(\mathbf{R}_n) \sum\limits_{jm} \mathbf{J}_{ij}(\mathbf{R}_n - \mathbf{R}_m)\mathbf{m}_j(\mathbf{R}_m)}}{\int \mathrm{d}\boldsymbol{\omega}_i^{\mathbf{R}_n}\, \mathrm{e}^{\beta_\mathrm{B} \mathbf{S}_i(\mathbf{R}_n) \sum\limits_{jm} \mathbf{J}_{ij}(\mathbf{R}_n - \mathbf{R}_m)\mathbf{m}_j(\mathbf{R}_m)}} \tag{105}$$

that the solution $\mathbf{m}_i(\mathbf{R}_n) = \mathbf{0}$ always exists, representing the disordered state. However, below a certain temperature, solutions with $\mathbf{m}_i(\mathbf{R}_n) \neq \mathbf{0}$ should exist. The temperature at which one of the solution goes to zero by increasing the temperature is called *branching temperature*, T_b. In the neighbourhood of T_b, the exponential function of the mean-field equation can be written in a linear form on $\mathbf{m}_i(\mathbf{R}_n)$. When the value of the average spin is small, only the first non-null term on the series development of the exponential functions is retained. We obtain the equations:

$$\sum_{jm} \mathbf{J}_{ij}(\mathbf{R}_n - \mathbf{R}_m)\mathbf{m}_j(\mathbf{R}_m) = -3k_\mathrm{B}T_\mathrm{b}\mathbf{m}_i(\mathbf{R}_n) \tag{106}$$

calling $\lambda = -3k_\mathrm{B}T_\mathrm{b}$, and making explicit the components of the exchange tensor, we obtain:

$$\sum_{jm\beta} J_{ij}^{\alpha\beta}(\mathbf{R}_n - \mathbf{R}_m) m_j^{\beta}(\mathbf{R}_m) = \lambda m_i^{\alpha}(\mathbf{R}_n) \tag{107}$$

Using the translational symmetry through the Fourier transform of the values $\mathbf{m}_j(\mathbf{R}_m)$ as:

$$\mathbf{m}_j(\mathbf{R}_m) = \sum_{\mathbf{k}} \mathbf{S}_{\mathbf{k}j}\, \mathrm{e}^{-2\pi\mathrm{i}\mathbf{k}\mathbf{R}_m} \tag{108}$$

where $\mathbf{S}_{\mathbf{k}j}$ represent the Fourier components of the magnetic moment. Notice that these complex vectors are defined for each atom j in a primitive cell taken as the origin cell (or *zero cell*). Replacing this value of the magnetic moment in the previous equation, we obtain a compact linear equation in the Fourier coefficients that reduces to an eigenvalue problem:

$$\sum_{jm} \mathbf{J}_{ij}(\mathbf{R}_n - \mathbf{R}_m) \sum_{\mathbf{k}} \mathbf{S}_{\mathbf{k}j}\, \mathrm{e}^{-2\pi\mathrm{i}\mathbf{k}\mathbf{R}_m} = \lambda \sum_{\mathbf{k}} \mathbf{S}_{\mathbf{k}i}\, \mathrm{e}^{-2\pi\mathrm{i}\mathbf{k}\mathbf{R}_n} \tag{109}$$

The sum over $\mathbf{k}$-vectors in both sides of the equations may be eliminated by imposing the equality of each term:

$$\sum_{jm} \mathbf{J}_{ij}(\mathbf{R}_n - \mathbf{R}_m)\mathbf{S}_{\mathbf{k}j}\, \mathrm{e}^{-2\pi\mathrm{i}\mathbf{k}\mathbf{R}_m} = \lambda \mathbf{S}_{\mathbf{k}i}\, \mathrm{e}^{-2\pi\mathrm{i}\mathbf{k}\mathbf{R}_n} \tag{110}$$

$$\sum_{jm} \mathbf{J}_{ij}(\mathbf{R}_n - \mathbf{R}_m)\, \mathrm{e}^{2\pi\mathrm{i}\mathbf{k}(\mathbf{R}_n - \mathbf{R}_m)} \mathbf{S}_{\mathbf{k}j} = \sum_{j} \sum_{p} \mathbf{J}_{ij}(\mathbf{R}_p)\, \mathrm{e}^{2\pi\mathrm{i}\mathbf{k}\mathbf{R}_p} \mathbf{S}_{\mathbf{k}j} = \lambda \mathbf{S}_{\mathbf{k}i} \tag{111}$$

The quantity obtained from the sum over p is the Fourier transform of the generalised exchange tensor parameters, and we call it:

$$\xi_{ij}^{\alpha\beta}(\mathbf{k}) = \sum_{p} J_{ij}^{\alpha\beta}(\mathbf{R}_p)\, \mathrm{e}^{2\pi\mathrm{i}\mathbf{k}\mathbf{R}_p} \tag{112}$$

$\xi_{ij}^{\alpha\beta}(\mathbf{k})$ is a matrix of dimension $3n_a \times 3n_a$, n_a being the number of magnetic atoms in a primitive unit cell. The problem of finding the first ordered state of a system of classical spins in the mean-field approximation has a general solution that has been reduced to an eigenvalue problem. The first ordered state is given by the eigenvector corresponding to the highest eigenvalue of the equation:

$$\sum_{j\beta} \xi_{ij}^{\alpha\beta}(\mathbf{k}) S_{\mathbf{k}j\beta} = \lambda S_{\mathbf{k}i\alpha} \tag{113}$$

In the case of isotropic exchange interactions, the Fourier transform is reduced to a matrix of dimension $n_a \times n_a$ and all the components of $\mathbf{S}_{\mathbf{k}i}$ satisfy a smaller eigenvalue equation

$$\sum_{j} \xi_{ij}(\mathbf{k}) \mathbf{S}_{\mathbf{k}j} = \lambda \mathbf{S}_{\mathbf{k}i} \tag{114}$$

The eigenvectors of (113) correspond to linear combinations of basis functions of the *irreps* of the group symmetry of the crystal structure that is implicitly embedded in the Fourier transform of the exchange interactions (112). Notice that single-ion anisotropy is included in the exchange parameters when $i = j$ and $\mathbf{R}_p = 0$.

Appendix D. Glossary

1. **Propagation (or modulation) vector** ($\mathbf{k}, \mathbf{q}$). The propagation vector $\mathbf{k}$ (or $\mathbf{k}$-vector for short) is a vector defined in reciprocal space that is used in Solid State Physics as a label for defining electron states in a solid. In the present context, it serves for indexing magnetic Bragg reflections or satellite reflections of a modulated structure. Modulated structures are normally characterised by a set of independent propagation vectors $\{\mathbf{k}_1, \mathbf{k}_2, \ldots, \mathbf{k}_d\}$ determining the dimension of the superspace $D = 3 + d$. The scattering vector corresponding to a Bragg reflection is given by: $\mathbf{h} = \mathbf{H} + \sum_{i=1}^{d} n_i \mathbf{k}_i$.
2. **Star of k** $\{\mathbf{k}\}$. When applying the point group operators of a space group to a primary $\mathbf{k}$-vector, we obtain a finite set of different $\mathbf{k}$-vectors constituting the *star* of the propagation vector $\{\mathbf{k}\} = \{g_1\mathbf{k}, g_2\mathbf{k} \ldots g_n\mathbf{k}\} = \{\mathbf{k}_1, \mathbf{k}_2 \ldots \mathbf{k}_m\}$. Notice that the number of generated $\mathbf{k}$-vectors, m, is generally smaller than the order n of the point group because, depending on the particular primary $\mathbf{k}$-vector, some operators may left it invariant (or equivalent to it).
3. **Polar vector**. Is a quantity defined in an n-dimensional space by n components P_i, $i = 1, 2, \ldots, n$ that transform under operations conserving distances and angles (orthogonal transformations), represented by a matrix of components A_{ij}, as $P'_i = \sum_{j=1}^{n} A_{ij} P_j$. Examples of polar vectors are: vector positions $\mathbf{r}$, linear momentum $\mathbf{p} = m\dot{\mathbf{r}}$, acceleration $\mathbf{a} = \ddot{\mathbf{r}}$, electric field $\mathbf{E}$, etc.
4. **Axial vector**. An axial vector is also-called *pseudo-vector* and it is defined by the transformation law $V'_i = \det(A) \times \sum_{j=1}^{n} A_{ij} V_j$, where $\det(A)$ is the determinant of the transformation matrix A. The determinant is equal to 1 for proper rotations and equal to -1 for improper rotations. Axial vectors in physics arise from the cross product of two polar vectors or by the curl of a polar vector field. Examples of axial vectors are: angular momentum $\mathbf{L} = \mathbf{r} \times \mathbf{p}$, magnetic field $\mathbf{B}$ (remember the third Maxwell equation in vacuum, using the velocity of light as unity: $\nabla \times \mathbf{E} = -\partial \mathbf{B}/\partial t$), magnetic moment $\mathbf{m}$, etc.
5. **Groups**. An abstract group is a set of elements $\mathcal{G} = \{g_1, g_2, \ldots, g_n\}$ in which an operation $\circ$ is defined such as $g_i \circ g_j = g_k \in \mathcal{G}$. It meets the following conditions: (*i*) the operation is associative $(g_i \circ g_j) \circ g_k = g_i \circ (g_j \circ g_k)$, (*ii*) there exists a *neutral* or *identity* element $e \in \mathcal{G}$, verifying $e \circ g_i = g_i \circ e = g_i$, and (*iii*) each element of the group has an *inverse* $g_i^{-1} \in \mathcal{G}$, verifying $g_i^{-1} \circ g_i = g_i \circ g_i^{-1} = e$.
6. **Point group**. A point group is a set of transformations that leave invariant a point in space. Normally, a point group is represented by a set of orthogonal matrices. The ordinary product of matrices is associative and all orthogonal matrices have an inverse equal to its transposed matrix, so the structure of the group is granted. Normally, the term point group is reserved to a finite group characterising the *symmetry* of an object in space.
7. **Space groups**. Combining point groups with groups of translations, it is possible to construct the so-called space groups. For making that possible, the existence of an underlying *lattice* defining the group of translations, which is always a subgroup of the space group, is necessary. A space group in 3D can be constructed only with crystallographic point groups (rotations of order 2, 3, 4 and 6 and their combination with the spatial inversion) in order to leave invariant the lattice. See section 7.1 for details.
8. **Superspace groups**. These are particular kind of space groups in n-dimensions. Their operators act in a $(3 + d)$-dimensional space. The superspace groups allow the description of aperiodic crystal and magnetic structures recovering the periodicity in a number of dimension equal to 3 plus the number of independent modulation vectors. See section 8.3 for details.
9. **Symmetry**. A symmetry is a transformation that leaves invariant an object. That means that the final object, after applying the transformation, is indistinguishable from the initial one. When speaking loosely about the *symmetry* of an object, it is understood that we refer to the group of symmetry of the object: the set of all transformations leaving invariant the object.
10. **Representation of a group**. A group is an abstract algebraic concept that makes reference to arbitrary elements without defining its physical nature. In physics and chemistry, group theory is of capital importance from many points of view. A representation of a group is a set of square matrices that is isomorphous to the abstract group. See section 7.1 for details.
11. **Irreducible representations**. A representation of dimension n (set of $n \times n$ matrices) can be *reduced* by a common similarity transformation ($\Gamma' = S\Gamma S^{-1}$) to a set of matrices having a block-diagonal structure. The submatrices having

the lower dimensions form also representations of the same group and they are called *irreducible representations* (*irreps*) when no further similarity transformation can be found to still reduce them. See section 7.1 for details.

References

[1] P. Curie, Propriétés des corps magnétiques à diverses températures, C. r. hebd. séances Acad. sci. 118 (1894) 1134 and references therein.
[2] P. Langevin, C. r. hebd. séances Acad. sci. 139 (1904) 1204–1206, Ann. Chim. Phys. 5 (1905) 70–127. The very short first article outlines the physical picture while the very long second one gives the details and the mathematical derivation.
[3] L. Brillouin, Les moments de rotation et le magnétisme dans la mécanique ondulatoire, J. Phys. Radium 8 (1927) 74–84, https://hal.archives-ouvertes.fr/jpa-00205282/document.
[4] L. Onsager, Crystal statistics. I. A two-dimensional model with an order-disorder transition, Phys. Rev. 65 (1944) 117–149;
B. Kaufman, Crystal statistics. II. Partition function evaluated by spinor analysis, Phys. Rev. 76 (1949) 1232–1243;
B. Kaufman, L. Onsager, Crystal statistics. III. Short-range order in a binary Ising lattice, Phys. Rev. 76 (1949) 1244–1252.
[5] L. Néel, Influence des fluctuations du champ moléculaire sur les propriétés magnétiques des corps, Ann. Phys. 17 (1932) 5–105;
Théorie du paramagnétisme constant ; application au manganèse, C. R. hebd. séances Acad. Sci. 203 (1936) 304–306.
[6] L.D. Landau, Eine mögliche Erklärung der Feldabhängigkeit der Suszeptibilität bei niedrigen Temperaturen, Phys. Z. Sowjetunion 4 (1933) 675, English translation: A possible explanation of the field dependence of the susceptibility at low temperatures, in: D. Ter Haar (Ed.), Collected Papers of L.D. Landau, Pergamon, Oxford, 1965, p. 73.
[7] C.G. Shull, J.S. Smart, Detection of antiferromagnetism by neutron diffraction, Phys. Rev. 76 (1949) 1256.
[8] C.G. Shull, E.O. Wollan, W.A. Strauser, Magnetic structure of magnetite and its use in studying the neutron magnetic interaction, Phys. Rev. 81 (1951) 483.
[9] F. de Bergevin, M. Brunel, Observation of magnetic superlattice peaks by X-ray diffraction on an antiferromagnetic NiO crystal, Phys. Lett. A 39 (1972) 141–142.
[10] F. de Bergevin, M. Brunel, Diffraction of X rays by magnetic crystals, Acta Crystallogr. A 37 (1981) 314–331.
[11] Y. Yafet, C. Kittel, Antiferromagnetic arrangements in ferrites, Phys. Rev. 87 (1952) 290.
[12] V. Baltz, A. Manchon, M. Tsoi, T. Moriyama, T. Ono, Y. Tserkovnyak, Antiferromagnetic spintronics, Rev. Mod. Phys. 90 (1) (2018) 015005.
[13] T. Riste, Magnetic scattering of neutrons in magnetite, J. Phys. Chem. Solids 17 (1961) 308.
[14] A. Yoshimori, A new type of antiferromagnetic structure in the rutile type crystal, J. Phys. Soc. Jpn. 14 (1959) 807.
[15] A. Herpin, P. Mériel, Étude de l'antiferromagnétisme hélicoïdal de $MnAu_2$ par diffraction de neutrons, J. Phys. Radium 22 (1961) 337.
[16] A. Herpin, P. Mériel, J. Villain, Structure magnétique de l'alliage $MnAu_2$, C. r. hebd. séances Acad. sci. 249 (1959) 1334.
[17] F. Bertaut, Configurations magnétiques, C. r. hebd. séances Acad. sci. 252 (1961) 76, 2078.
[18] F. Bertaut, Sur la théorie de l'ordre magnétique, C. r. hebd. séances Acad. sci. 258 (1964) 3835.
[19] J. Villain, La structure des substances magnétiques, J. Phys. Chem. Solids 11 (1961) 303.
[20] W. Heisenberg, Zur Theorie des Ferromagnetismus, Z. Phys. 49 (1928) 619–636.
[21] M.A. Rudermann, C. Kittel, Indirect exchange coupling of nuclear magnetic moments by conduction electrons, Phys. Rev. 96 (1954) 99.
[22] J. Villain, M. Lavagna, P. Bruno, Jacques Friedel et la théorie des métaux et alliages, C. R. Physique 17 (2016) 276–290.
[23] D. Émile, How the Friedel oscillations entered the physics of metallic alloys, C. R. Physique 17 (2016) 291–293.
[24] P. Mallet, I. Brihuega, V. Cherkez, J. Marìa Gómez-Rodríguez, J.-Y. Veuillen, Friedel oscillations in graphene-based systems probed by scanning tunneling microscopy, C. R. Physique 17 (2016) 294–301.
[25] C. Bena, Friedel oscillations: decoding the hidden physics, C. R. Physique 17 (2016) 302–321.
[26] R.J. Elliott (Ed.), Magnetic Properties of Rare-Earth Metals, Plenum Press, New York, 1972.
[27] J. Rossat-Mignod, P. Burlet, J. Villain, H. Bartholin, W. Tcheng-Si, D. Florence, O. Vogt, Phase diagram and magnetic structures of CeSb, Phys. Rev. B 16 (1977) 440.
[28] J. Rossat-Mignod, Magnetic structures, in: Methods of Experimental Physics: Neutron Scattering, vol. 3, Academic Press, 1987.
[29] I.E. Dzyaloshinskii, Thermodynamical theory of 'weak' ferromagnetism in antiferromagnetic substances, Zh. Eksp. Teor. Fiz. 32 (1957) 1547, Sov. Phys. JETP 5 (1957) 1259.
[30] T. Moriya, Anisotropic superexchange interaction and weak ferromagnetism, Phys. Rev. 120 (1961) 91.
[31] Y. Frenkel, T. Kontorova, On the theory of plastic deformation and doubling, Zh. Eksp. Teor. Phys. 8 (89) (1938) 1340, 1349.
[32] M. Peyrard, S. Aubry, Critical behaviour by breaking of analyticity in the discrete Frenkel–Kontorova model, J. Phys. C 16 (1983) 1593.
[33] J. Villain, M.B. Gordon, The Devil's staircase and harmless staircase, J. Phys. C 15 (1980) 3117–3134.
[34] M.T. Freiser, Thermal variation of the pitch of helical spin configurations, Phys. Rev. 123 (1961) 2003.
[35] T.M. Luttiger, L. Tisza, Theory of dipole interaction in crystals, Phys. Rev. 70 (1954) 954.
[36] T.A. Kaplan, Classical spin-configuration stability in the presence of competing exchange forces, Phys. Rev. 116 (1959) 888.
[37] T.A. Kaplan, D.H. Lyons, Method for determining ground-state spin configurations, Phys. Rev. 120 (1960) 1580.
[38] M.E. Zhitomirsky, A. Honecker, O.A. Petrenko, Field induced ordering in highly frustrated antiferromagnets, Phys. Rev. Lett. 85 (2000) 3269.
[39] T. Coletta, T.A. Toth, K. Penc, F. Mila, Semiclassical theory of the magnetization process of the triangular lattice Heisenberg model, Phys. Rev. B 94 (2016) 075136.
[40] E.F. Bertaut, Representation analysis of magnetic structures, Acta Crystallogr. A 24 (1968) 217.
[41] J. Rodríguez-Carvajal, F. Bourée, Symmetry and magnetic structures, in: B. Grenier, V. Simonet, H. Schober (Eds.), Contribution of Symmetries in Condensed Matter, in: EPJ Web of Conferences, vol. 22, 2012, 00010.
[42] A.H. Hill, et al., Neutron diffraction study of mesoporous and bulk hematite, α–Fe_2O_3, Chem. Mater. 20 (2008) 4891.
[43] Y.A. Izyumov, V.E. Naish, R.P. Ozerov, Neutron Diffraction of Magnetic Materials, Consultants Bureau, Plenum Publishing Corporation, New York, 1991.
[44] I. Mirebeau, et al., Ordered spin ice state and magnetic fluctuations in $Tb_2Sn_2O_7$, Phys. Rev. Lett. 94 (2005) 246402.
[45] E. Fawcett, Spin-density-wave antiferromagnetism in chromium, Rev. Mod. Phys. 60 (1988) 209–283.
[46] J.P. Hill, G. Helgesen, D. Gibbs, X-ray-scattering study of charge- and spin-density waves in chromium, Phys. Rev. B 51 (1995) 10336–10344.
[47] M. Kenzelmann, A.B. Harris, S. Jonas, C. Broholm, J. Schefer, S.B. Kim, C.L. Zhang, S.-W. Cheong, O.P. Vajk, J.W. Lynn, Magnetic inversion symmetry breaking and ferroelectricity in $TbMnO_3$, Phys. Rev. Lett. 95 (2005) 087206.
[48] C.G. Shull, E.O. Wollan, W.C. Koehler, Neutron scattering and polarisation by ferromagnetic materials, Phys. Rev. 84 (1951) 912.
[49] M. Blume, Polarisation effects in the magnetic elastic scattering of slow neutrons, Phys. Rev. 130 (1963) 1670.
[50] S.V. Maleyev, V.G. Baryakhtar, R.A. Suris, Fiz. Tverd. Tela 4 (1962) 3461, English translation: Sov. Phys., Solid State 4 (1963) 2533.
[51] R.M. Moon, T. Riste, W.C. Koehler, Polarisation analysis of thermal-neutron scattering, Phys. Rev. 181 (1969) 920.
[52] S.W. Lovesey, Theory of Neutron Scattering from Condensed Matter, Oxford University Press, 1984.
[53] E. Ressouche, Polarized neutron diffraction, Collect. SFN 13 (2014) 02002, https://doi.org/10.1051/sfn/20141302002, Owned by the authors, published by EDP Sciences, 2014.

[54] J.B. Forsyth, P.J. Brown, The spatial distribution of magnetisation density in Mn_5Ge_3, J. Phys. Condens. Matter 2 (11) (1990) 2713.
[55] P.J. Brown, K.U. Neumann, P.J. Webster, K.R.A. Ziebeck, The magnetization distributions in some Heusler alloys proposed as half-metallic ferromagnets, J. Phys. Condens. Matter 12 (2000) 1827.
[56] P.J. Brown, J.B. Forsyth, F. Tasset, Neutron polarimetry, Proc. R. Soc. Lond. A 442 (1993) 147–160.
[57] P.J. Brown, T. Chattopadhyay, J.B. Forsyth, V. Nunez, F. Tasset, Antiferromagnetism in CuO studied by neutron polarimetry, J. Phys. Condens. Matter 3 (1991) 4281–4287.
[58] F. Tasset, P.J. Brown, E. Lelievre-Berna, T. Roberts, S. Pujol, J. Allibon, E. Bourgeat-Lami, Spherical neutron polarimetry with Cryopad-II, Physica B 267–268 (1999) 69–74.
[59] P.J. Brown, T. Chatterji, Neutron diffraction and polarimetric study of the magnetic and crystal structures of $HoMnO_3$ and $YMnO_3$, J. Phys. Condens. Matter 18 (2006) 10085.
[60] T. Nagamiya, Helical spin ordering, in: F. Seitz, D. Turnbull, H. Ehrenreich (Eds.), Solid State Physics, vol. 20, Academic Press, New York, 1967, pp. 305–411.
[61] E.F. Bertaut, Spin configurations of ionic structures. Theory and practice, in: G.T. Rado, H. Shul (Eds.), Magnetism, vol. III, Academic Press, New York, 1963, p. 149, Ch. 4. See also Acta Crystallogr. A 24 (1968) 217, J. Phys. Colloques 32 (1971) C1-462-C1-470, J. Magn. Magn. Mater. 24 (1981) 267.
[62] Y.A. Izyumov, V.E. Naish, Symmetry analysis in neutron diffraction studies of magnetic structures: 1. A phase transition concept to describe magnetic structures in crystals, J. Magn. Magn. Mater. 12 (1979) 239;
Y.A. Izyumov, V.E. Naish, V.N. Syromiatnikov, Symmetry analysis in neutron diffraction studies of magnetic structures: 2. Changes in periodicity at magnetic phase transitions, J. Magn. Magn. Mater. 12 (1979) 249;
Y.A. Izyumov, V.E. Naish, S.B. Petrov, Symmetry analysis in neutron diffraction studies of magnetic structures: 3. An example: the magnetic structure of spinels, J. Magn. Magn. Mater. 13 (1979) 267–274;
Y.A. Izyumov, V.E. Naish, S.B. Petrov, Symmetry analysis in neutron diffraction studies of magnetic structures: 4. Theoretical group analysis of exchange Hamiltonian, J. Magn. Magn. Mater. 13 (1979) 275.
[63] J. Schweizer, F. Givord, J-X. Boucherle, F. Bourdarot, E. Ressouche, The accurate magnetic structure of $CeAl_2$ at various temperatures in the ordered state, J. Phys. Condens. Matter 20 (2008) 135204.
[64] E. Garcia-Matres, J.L. Martinez, J. Rodriguez-Carvajal, Neutron diffraction study of the magnetic ordering in the series R_2BaNiO_5 (R = rare earth), Eur. Phys. J. B 24 (2001) 59–70, https://doi.org/10.1007/s100510170022.
[65] J.A. Lim, E. Blackburn, G. Beutier, F. Livet, N. Magnani, A. Bombardi, R. Caciuffo, G.H. Lander, Coherent magnetic diffraction from the uranium M4 edge in the multi-k magnet, USb, J. Phys. Conf. Ser. 519 (2014) 01201.
[66] J. Rodríguez-Carvajal, Physica B 192 (1993) 55. Programs of the FullProf suite can be freely downloaded from https://www.ill.eu/sites/fullprof/.
[67] P. Schobinger-Papamantellos, J. Rodríguez-Carvajal, G. André, K.H.J. Buschow, Re-entrant ferrimagnetism in $TbMn_6Ge_6$, J. Magn. Magn. Mater. 150 (1995) 311.
[68] D.H. Lyons, T.A. Kaplan, K. Dwight, N. Menyuk, Classical theory of the ground spin-state in cubic spinels, Phys. Rev. 126 (2) (1962) 540.
[69] P. Dalmas de Réotier, A. Maisuradze, A. Yaouanc, B. Roessli, A. Amato, D. Andreica, G. Lapertot, Determination of the zero-field magnetic structure of the helimagnet MnSi at low temperature, Phys. Rev. B 93 (2016) 144419.
[70] A. Yaouanc, P. Dalmas de Reotier, A. Maisuradze, B. Roessli, Magnetic structure of the MnGe helimagnet and representation analysis, Phys. Rev. B 95 (2017) 174422.
[71] C. Bradley, A. Cracknell, The Mathematical Theory of Symmetry in Solids, Oxford University Press, 1972.
[72] A. Schoenflies, Krystallsysteme und Krystallstructur, Teubner, Leipzig, 1891.
[73] International Tables for Crystallography, Volume A, Space-Group Symmetry, 2016, https://doi.org/10.1107/97809553602060000114.
[74] H. Heesch, Zur systematischen Strukturtheorie II, Z. Kristallogr. 72 (1929) 177–201.
[75] N.V. Belov, N.N. Neronova, T.S. Smirnova, Tr. Inst. Krist. Akad. SSSR 11 (1955) 33–67, English translation in Sov. Phys. Crystallogr. 1 (1957) 487–488.
[76] A.M. Zamorzaev, Generalization of Fedorov groups, Kristallografiya 2 (1957) 15–20, English translation in Sov. Phys. Crystallogr. 2 (1957) 10–15.
[77] W. Opechowski, R. Guccione, Magnetic symmetry, in: G.T. Rado, H. Shull (Eds.), Magnetism, vol. II A, Academic Press, New York, 1965, p. 105, Ch. 3.
[78] V.A. Koptsik, Sov. Phys. Crystallogr. 12 (5) (1968) 723;
V.A. Koptsik, Shubnikov groups, in: Handbook on the Symmetry and Physical Properties of Crystal Structures, Izd. MGU, Moscow, 1966 (in Russian), English translation of text: J. Kopecky, B.O. Loopstra, Fysica Memo 175, Stichting, Reactor Centrum Nederland, 1971.
[79] D.B. Litvin, Magnetic space-group types, Acta Crystallogr. A 57 (2001) 729–730.
[80] Magnetic Space Groups, compiled by H.T. Stokes and B.J. Campbell, Department of Physics and Astronomy, Brigham Young University, Provo, Utah, USA. The last version of the tables date from June 2010. The tables can be found at http://stokes.byu.edu/iso/magneticspacegroups.php.
[81] P.M. de Wolff, The pseudo-symmetry of modulated crystal structures, Acta Crystallogr. A 30 (1974) 777–785.
[82] P.M. de Wolff, Symmetry operations for displacively modulated structures, Acta Crystallogr. A 33 (1977) 493–497.
[83] P.M. de Wolff, T. Janssen, A. Janner, The superspace groups for incommensurable crystal structures with a one-dimensional modulation, Acta Crystallogr. A 37 (1981) 625–636.
[84] A. Janner, T. Janssen, Symmetry of incommensurable crystal phases. I. Commensurate basic structures, Acta Crystallogr. A 36 (1980) 399–408 (and 408–415).
[85] T. Janssen, A. Janner, A. Looijenga-Vos, P. de Wolf, Incommensurable and commensurable modulated structures, in: International Tables for Crystallography, vol. C, Kluwer, Amsterdam, 2006, pp. 907–955, Ch. 9.8.
[86] T. Janssen, G. Chapuis, M. de Boissieu, Aperiodic Crystals: From Modulated Phases to Quasicrystals, Oxford University Press, 2007.
[87] S. van Smaalen, Incommensurable Crystallography, Oxford University Press, Oxford, 2007.
[88] J.M. Perez-Mato, J.L. Ribeiro, V. Petricek, M.I. Aroyo, Magnetic superspace groups and symmetry constraints in incommensurable magnetic phases, J. Phys. Condens. Matter 24 (2012) 163201.
[89] A. Yamamoto, Structure factor of modulated crystal structures, Acta Crystallogr. A 38 (1982) 87–92.
[90] H.T. Stokes, B.J. Campbell, S. van Smaalen, Generation of $(3+d)$-dimensional superspace groups for describing the symmetry of modulated crystalline structures, Acta Crystallogr. A 67 (2011) 45–55.
[91] T. Janssen, A. Janner, Aperiodic crystals and superspace concepts, Acta Crystallogr. B 70 (2014) 617–651.
[92] J.M. Perez-Mato, G. Madariaga, F.J. Zuniga, A. Garcia-Arribas, On the structure and symmetry of incommensurable phases. A practical formulation, Acta Crystallogr. A 43 (1987) 216–226.
[93] N. Terada, D.D. Khalyavin, J.M. Perez-Mato, P. Manuel, D. Prabhakaran, A. Daoud-Aladine, P.G. Radaelli, H.S. Suzuki, H. Kitazawa, Magnetic and ferroelectric orderings in multiferroic α-$NaFeO_2$, Phys. Rev. B 89 (2014) 184421.
[94] H.M. Rietveld, A profile refinement method for nuclear and magnetic structures, J. Appl. Crystallogr. 2 (1969) 65.
[95] A.W. Hewat, Atomic Energy Research Establishment, Report AERE-R7350, Harwell, Oxfordshire, UK, 1973.
[96] J.C. Matthewman, P. Thomson, P.J. Brown, The Cambridge Crystallography Subroutine Library, J. Appl. Crystallogr. 15 (1982) 167–173. The last version of the library can be downloaded from https://forge.epn-campus.eu/projects/sxtalsoft/repository/show/CCSL.
[97] L.B. McCusker, R.B. Von Dreele, D.E. Cox, D. Louer, P. Scardi, Rietveld refinement guidelines, J. Appl. Crystallogr. 32 (1999) 36–50.

[98] B.H. Toby, R.B. Von Dreele, GSAS-II: the genesis of a modern open-source all purpose crystallography software package, J. Appl. Crystallogr. 46 (2013) 544–549. The programs can be downloaded from www.ncnr.nist.gov/xtal/software/gsas.html.
[99] F. Izumi, T. Ikeda, A Rietveld-analysis program RIETAN-98 and its applications to zeolites, Mater. Sci. Forum 321–324 (2000) 198–205.
[100] F. Izumi, K. Momma, Three-dimensional visualization in powder diffraction, Solid State Phenom. 130 (2007) 15–20.
[101] A.A. Coelho, TOPAS and TOPAS-Academic: an optimization program integrating computer algebra and crystallographic objects written in C++, J. Appl. Crystallogr. 51 (2018) 210–218.
[102] J.K. Maichle, J. Ihringer, W. Prandl, Simultaneous structure refinement of neutron, synchrotron and X-ray powder diffraction patterns, J. Appl. Crystallogr. 21 (1988) 22–27.
[103] D.B. Wiles, R.A. Young, A new computer-program for Rietveld analysis of x-ray-powder diffraction patterns, J. Appl. Crystallogr. 14 (1981) 149–151.
[104] W. Sikora, F. Bialasb, L. Pytlik, MODY: a program for calculation of symmetry-adapted functions for ordered structures in crystals, J. Appl. Crystallogr. 37 (2004) 1015–1019.
[105] A.S. Wills, A new protocol for the determination of magnetic structures using Simulated Annealing and Representational Analysis-SARAh, Physica B 276 (2000) 680–681.
[106] J. Rodriguez-Carvajal, A program for calculating irreducible representation of little groups and basis functions of polar and axial vector properties, Laboratoire Léon-Brillouin, 2004, unpublished.
[107] M.I. Aroyo, J.M. Perez-Mato, D. Orobengoa, E. Tasci, G. de la Flor, A. Kirov, Crystallography online: Bilbao Crystallographic Server, Bulg. Chem. Commun. 43 (2) (2011) 183–197;
M.I. Aroyo, J.M. Perez-Mato, C. Capillas, E. Kroumova, S. Ivantchev, G. Madariaga, A. Kirov, H. Wondratschek, Bilbao Crystallographic Server I: databases and crystallographic computing programs, Z. Kristallogr. 221 (1) (2006) 15–27, https://doi.org/10.1524/zkri.2006.221.1.15;
M.I. Aroyo, A. Kirov, C. Capillas, J.M. Perez-Mato, H. Wondratschek, Bilbao Crystallographic Server II: representations of crystallographic point groups and space groups, Acta Crystallogr. A 62 (2006) 115–128, https://doi.org/10.1107/S0108767305040286;
The web page is http://www.cryst.ehu.es.
[108] J.M. Perez-Mato, S.V. Gallego, E.S. Tasci, L. Elcoro, G. de la Flor, M.I. Aroyo, Symmetry-based computational tools for magnetic crystallography, Annu. Rev. Mater. Res. 45 (2015) 217–248.
[109] S.V. Gallego, J. Manuel Perez-Mato, L. Elcoro, E.S. Tasci, R.M. Hanson, K. Momma, M.I. Aroyo, G. Madariaga, MAGNDATA: towards a database of magnetic structures. I. The commensurable case, J. Appl. Crystallogr. 49 (2016) 1750–1776.
[110] S.V. Gallego, J. Manuel Perez-Mato, L. Elcoro, E.S. Tasci, R.M. Hanson, K. Momma, M.I. Aroyo, G. Madariaga, MAGNDATA: towards a database of magnetic structures. II. The incommensurable case, J. Appl. Crystallogr. 49 (2016) 1941–1956.
[111] D. Gezelter, B.A. Smith, E. Willighagen, et al., An interactive viewer for three-dimensional chemical structures. This is an open source project initiated by end of the nineties with many contributors. The web page is http://jmol.sourceforge.net.
[112] A. Yamamoto, The programs REMOS and PREMOS, in: J.M. Perez-Mato, F.J. Zuniga, G. Madariaga (Eds.), Methods of Structural Analysis of Modulated Structures and Quasicrystals, World Scientific, Singapore, 1991, pp. 249–261.
[113] V. Petricek, M. Dusek, L. Palatinus, Crystallographic computing system JANA2006: general features, Z. Kristallogr. 229 (5) (2014) 345–352, https://doi.org/10.1515/zkri-2014-1737.
[114] B.J. Campbell, H.T. Stokes, D.E. Tanner, D.M. Hatch, ISODISPLACE: a web-based tool for exploring structural distortions, J. Appl. Crystallogr. 39 (2006) 607–614.
[115] H.T. Stokes, et al., ISOTROPY Software Suite (1984–2013). The programs, resources and references can be found at the web site http://stokes.byu.edu/iso/isotropy.php.
[116] H.T. Stokes, B.J. Campbell, R. Cordes, Tabulation of irreducible representations of the crystallographic space groups and their superspace extensions, Acta Crystallogr. A 69 (2013) 388–395.
[117] F. Damay, Neutrons and magnetic structures: analysis methods and tools, J. Phys. D, Appl. Phys. 48 (2015) 504005.
[118] N. Qureshi, Mag2Pol: a program for the analysis of spherical neutron polarimetry, flipping ratio and integrated intensity data, J. Appl. Crystallogr. 52 (2019) 175–185.
[119] N.A. Katcho, J. Rodriguez-Carvajal, A program for generating and identify arbitrary settings of general crystallographic groups, 2019, unpublished.
[120] Commission on Magnetic Structures of the International Union of Crystallography, http://magcryst.org/.